AFIT/GE/ENG/99M-27

Loop Gain Estimation for Adaptive Control

THESIS

Jamey P. Sillence B.S.E.E.
Second Lieutenant, USAF

AFIT/GE/ENG/99M-27

Disclaimer

The views expressed in this dissertation are those of the author and do not reflect the official policy or position of the United States Air Force, the Department of Defense, or the United States Government.

AFIT/GE/ENG/99M-27

Loop Gain Estimation for Adaptive Control

THESIS

Presented to the Faculty of the Graduate School of Engineering of the Air Force Institute of Technology Air University In Partial Fulfillment for the Degree of

Masters of Science

Specialization in: Electrical Engineering

Jamey P. Sillence B.S.E.E.

Second Lieutenant, USAF

Air Force Institute of Technology

Wright-Patterson AFB, Ohio

March, 1999

Sponsored in part by AFRL/VAAD

AFIT/GE/ENG/99M-27

Loop Gain Estimation for Adaptive Control

Jamey P. Sillence B.S.E.E.

Second Lieutenant, USAF

Approved:

M. Pachter — March 5, 1999

Dr. Meir Pachter
Committee Chairman

Date

Peter S. Maybeck — 5 Mar 99

Dr. Peter Maybeck
Committee member

Date

Dedication

I dedicate this work to my wife Cathy. Her understanding and support encouraged me and her smile let me know there is life after thesis.

Acknowledgments

I would like to thank the faculty of the Guidance and Control Department for their knowledge and motivation. I would especially like to thank my advisor, Dr. Pachter for sparking my interest in this thesis and providing constant direction and support and Dr. Maybeck for being my reader.

I would also like to thank my fellow classmates, Stephan Chastain, Ken Fisher, Andrew Proud, Barry Vanek, and Brian Young, for their insight, discussion, and being there when I had a question.

Table Of Contents

List of Figures

Page

Page

Page

List of Tables

List of Symbols

English Symbols

Symbol	Definition
q	Pitch rate
$\triangleq$	Defined as
$\equiv$	Equivalent to
n, m	Dimensions of a vector
$E(\cdot)$	Expectation operator
$\mathcal{R}$	All real numbers

Vectors/Matrices

Matrices	Upper case letters, A
Vectors	Lower case letters, b

Greek Symbols

Symbol	Definition
α	Angle of attack
Γ	Noise matrix

Subscripts

Symbol	Definition
k	Time increment
x	Related to parameters α and q

K	Related to critical loop gain, K
$(\cdot)_o$	Initial parameter

Superscript

Symbol	Definition
$(\cdot)^T$	Transpose
$(\cdot)^{-1}$	Inverse
$(\cdot)^n$	To the power of n

Abstract

The identification of a linear discrete-time control system's loop gain is addressed. The classical Kalman filter theory for state estimation in linear control systems is extended, and the control system's loop gain and state are jointly estimated. A rigorous analysis of the measurement situation under consideration yields explicit formulae for the loop gain's unbiased estimate and estimation error's covariance.

Loop Gain Estimation for Adaptive Control

Chapter 1 - Introduction

1.1 Background

Feedback, and the reliance on high gain action, are used to mitigate the ill effects of the unstructured environment where the controlled plant is operating. At the same time, the benefits of feedback control, and, in particular, high gain action, are severely circumscribed by sensor noise [10]. System identification entails the estimation of a control system's parameters from measurements on the system's inputs and outputs [11]; as such, system identification lends itself well to integration into modern feedback control synthesis, because no additional hardware, i.e., sensor or actuators, above and beyond the components used in conventional feedback control, are required. The incorporation of system identification into feedback control law synthesis calls for additional signal processing, however, a reduction in plant uncertainty is achieved. Therefore, lower gains in the feedback control law are possible. Hence, there is a strong incentive for the incorporation of system identification into control law synthesis and the employment of indirect adaptive control. Unfortunately, system identification, which entails the estimation of all the plant's parameters, resides in the realm of nonlinear filtering. It is however recognized that accurate information on the control matrix parameters is of paramount importance in control law design, e.g., in flight control one then refers to the "control derivatives". Now, in linear control systems, and provided that the dynamics matrix is known, the exclusive estimation of the parameters of the control matrix only is reducible to a problem in linear regression and therefore, is amenable to analysis using linear mathematics. Hence, a rigorous, i.e., an unbiased, estimate of the parameters of the control matrix

can be obtained. In this thesis, a simplified version of this problem is addressed and an algorithm for the estimation of a single input control system's critical loop gain parameter is developed. The inclusion of a "forgetting factor" into this basic algorithm, or the employment of a sliding window, will afford on-line operation. Thus, a possible mechanization of an indirect adaptive flight control system which incorporates the loop gain identification algorithm developed in this paper is illustrated in Fig 1. In a flight control application, the states α and q represent the aircraft's angle of attack and pitch rate, respectively.

1.2 Problem Statement

The linear discrete-time control system is considered,

$$x_{k+1} = Ax_k + Kbu_k + \Gamma w_k, \quad k = 0, 1, ..., N-1, \quad E(w_k w_k^T) = Q \tag{1}$$

$$x_o = N(\overline{x}_o, P_{ox}) \tag{2}$$

$$K = N(K_o, P_{o_K}) \tag{3}$$

$$y_{k+1} = Cx_{k+1} \tag{4}$$

$$z_{k+1} = y_{k+1} + v_{k+1}, \quad E(v_{k+1} v_{k+1}^T) = R \tag{5}$$

In the special case of a single scalar output, the measurement equation (5) is

$$z_{k+1} = y_{k+1} + v_{k+1}, \qquad v_{k+1} = N(0, \sigma^2) \tag{6}$$

The control system's state $x_k \in \Re^n$. The dynamics matrix A, the control matrix b, the observation matrix C and the vector Γ are known. The respective process and sensor noise covarinaces, Q and R (or σ) are also known. In addition, the prior information specified in Eqs. (2) and (3) is provided. It is required to identify the scalar loop gain K, given the input sequence $u_0, u_1, ..., u_{N-1}$ and the measurements record $z_1, z_2, ..., z_N$. An estimate of the control system's state is also obtained. Here, the loop gain parameter K is developed. Hence, for instance, in the flight control

application, one can now handle control surface failure. Obviously, for an unfailed plant (aircraft) the loop gain $K = 1$ (by definition), viz., K is unity, until a failure at time t_f reduces the control derivative and forces $K < 1$.

In this research, the identification of the control system's loop gain K is undertaken. The classical Kalman filter theory for linear control systems [3] is extended and the control system's state and loop gain are jointly estimated. Explicit formulae for the loop gain's (unbiased) estimate and estimation error covariance are derived. The state estimate and the covariance of the state estimation error are also obtained. Also, digital control and digital signal processing are employed. Thus, a sampling rate of 100Hz is used and in our simulation the continuous-time plant dynamics are discretized accordingly.

1.3 Proposed Adaptive Plant Controller

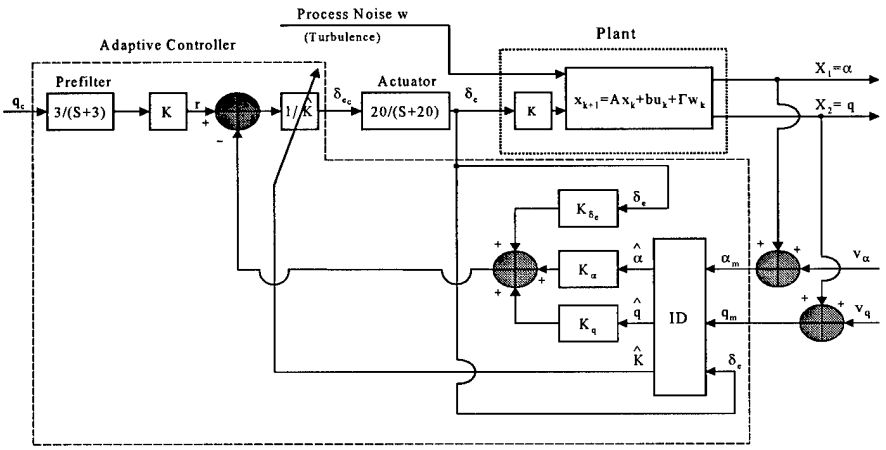

Figure 1. Flight Control System

The propsed adaptive controller is shown in Fig. 1. A pilot commands a pitch rate signal, q_c, into the adaptive controller. The commanded input is passed through a low pass filter and into a

PI or proportional fixed controller to imporve tracking performance creating the signal, r. Inside the boxed-off section labeled 'adaptive controller' is the system identification algorithm. The identification algorithm, i.e., modified Kalman filter, is fed noise corrupted measurements, α_m and q_m, from the plant. In turn, (filtered) estimates of α, q and loop gain K, $\hat{\alpha}$, $\hat{q}$ and $\hat{K}$ respectively, are calculated for each time sample. The estimates $\hat{\alpha}$ and $\hat{q}$ are then fed back and summed with the signal r. The reciprocal of $\hat{K}$ is fed back into the foward path after the summing junction of the states and signal r but before the actuator. The actuator being used in this research is for the elevator of an F-16 class aircraft. By feeding back $\frac{1}{\hat{K}}$, the effects of K in Eq. 1 will be reduced and tracking performance restored. The value of K corresponds to a degree of failure in the flight control system.

1.4 Assumptions

Chapter 2 describes the classical system ID procedure for finding a system model. For this thesis, the system order and plant is assumed to be known before hand. The research proceeds under the assumption that the failure in the elevator does not significantly change the over-all aircraft system model. For this reason, the identification of the aircraft model is not needed and the focus is spent of identifying the open-loop gain which corresponds to the degree of failure.

In this thesis, only the short period approximation is used and the phugoid period is neglected. This is done because the phugoid oscillation occurs in under thirty seconds where as the short period ocsillation occurs in under one second. Since the research being presented in this thesis deals with failing control surfaces, the time needed to detect a failure must occur in a short period of time. This is to prevent aircraft uncontrolability and loss.

When dealing with the short period approximation of an F-16 class aircraft, both the alpha and q channels are used in the feedback design - see Fig. 2 for a visual description of alpha.

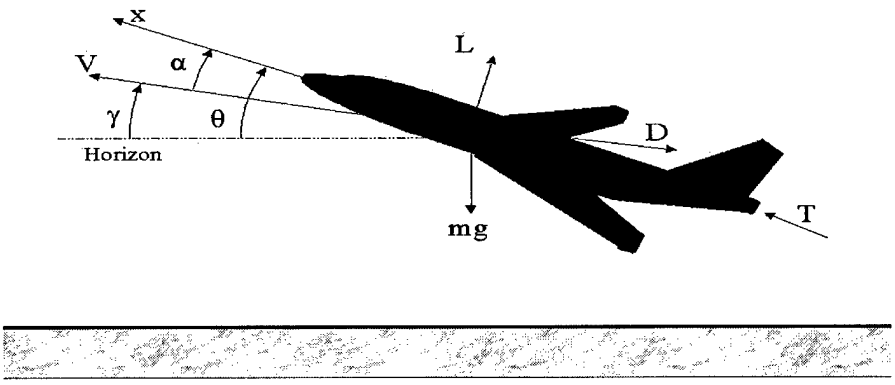

Figure 2. Aircraft longitudinal parameters

Although pitch rate tracking can be done without use of the alpha channel, Figs. 3-6, the extra data it provides is beneficial to the Kalman filter used in the system identification algorithm. It also provides additional tracking stability when there is a control surface failure in the longitudinal axis.

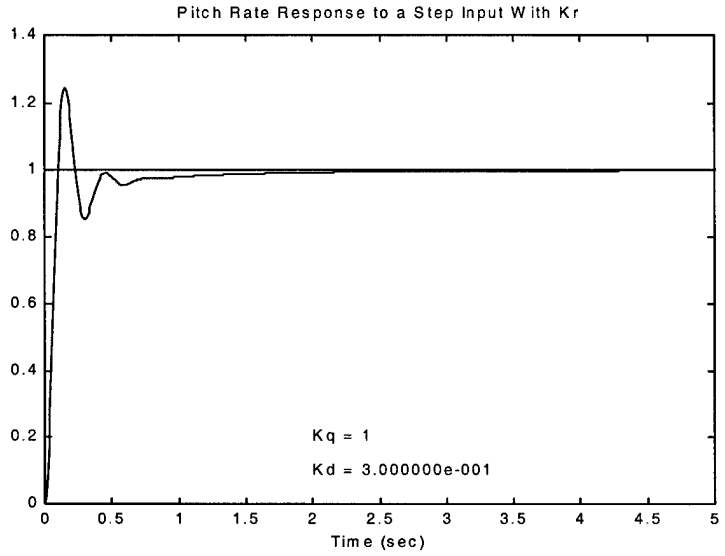

Figure 3. Pitch rate response without using alpha feedback with gain Kr

Figs. (7) and (8) show that a change in the measurement noise in the α channel has minimal effect on the controllers ability to track α (the dashed verticle line indicates the time of failure, $t = 3$ sec.). However, it does influence the pitch rate measurements -see Figs (9) and (10). This is because the two channels are coupled. For this reason, the square root of the strength of the alpha noise is held constant at 0.03 degrees. This way the effects of measurement noise on the controllers' ability to track the pitch rate can be analyzed and compared. It also provides some dynamics for the system identification algorithm and creates a more realistic measurement case. Implementing a PI or proprotional controller to improve tracking performance yielded similar results. This is due to the robustness of the original flight control system.

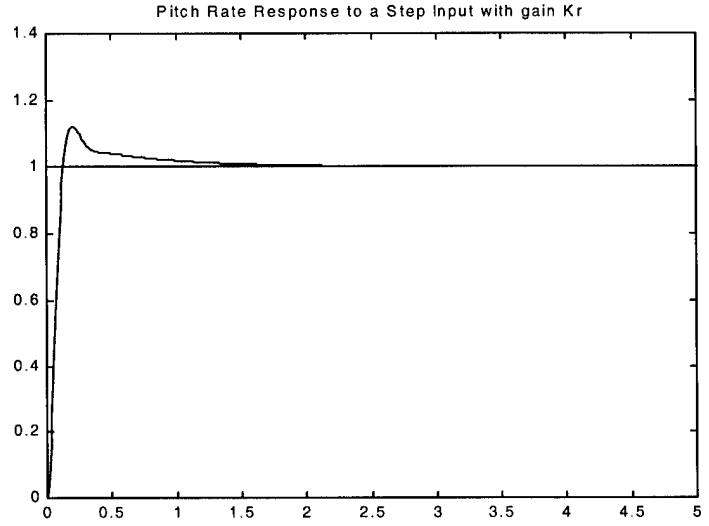

Figure 4. Pitch rate response with alpha feedback using gain Kr

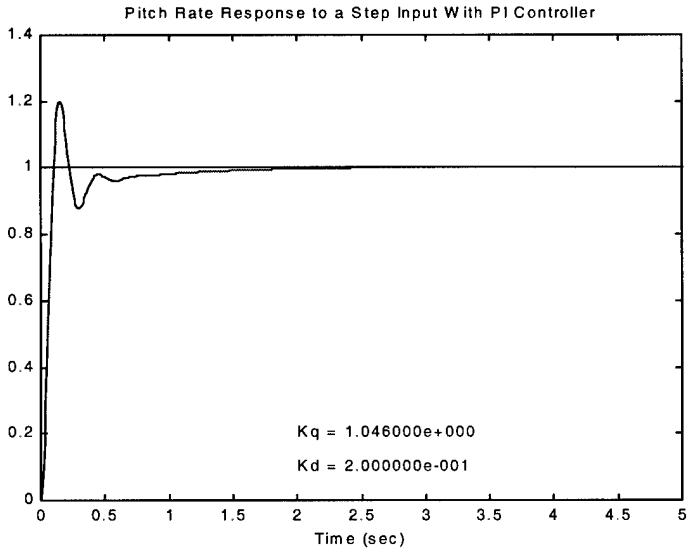

Figure 5. Pitch rate response without alpha feedback using a PI controller

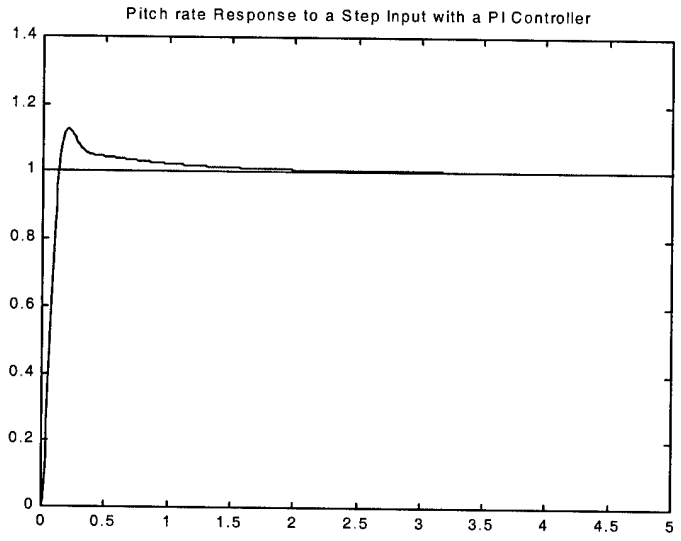

Figure 6. Pitch rate response with alpha feedback using a PI controller

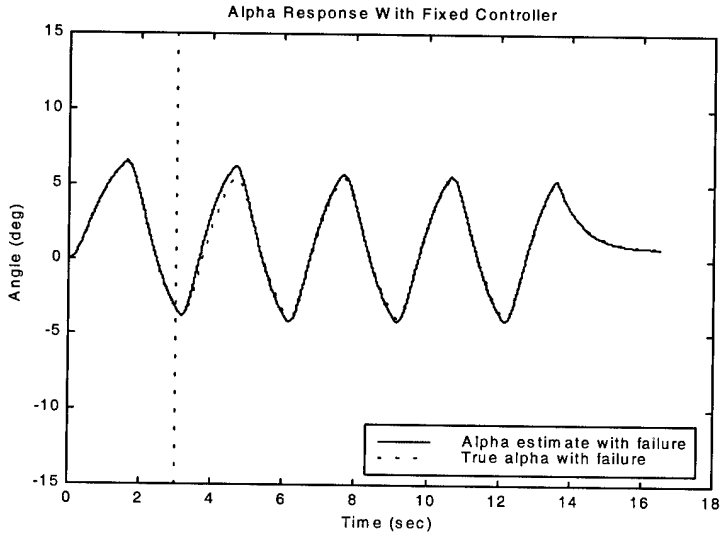

Figure 7. Alpha response with a fixed controller; $\sigma_\alpha = 0.03$ deg/sec, K=0.8, SNR=18.61 dB.

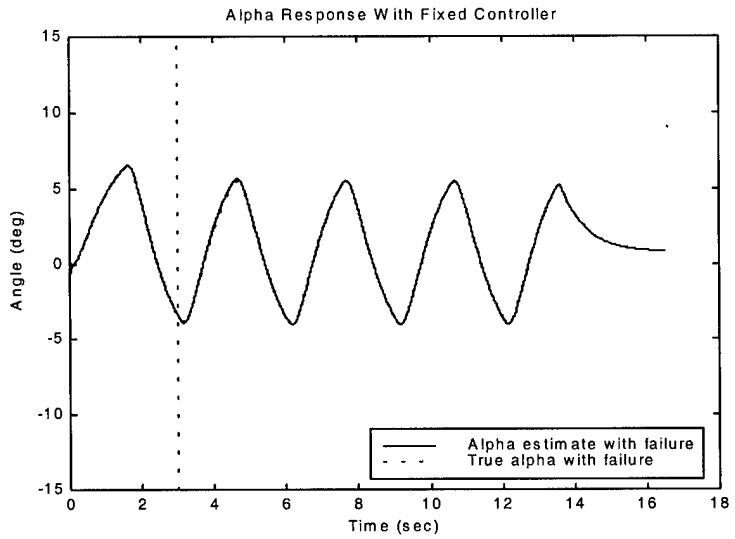

Figure 8. Alpha response with a fixed controller; $\sigma_\alpha = 0.3$ deg/sec, K=0.8, SNR=18.61 dB.

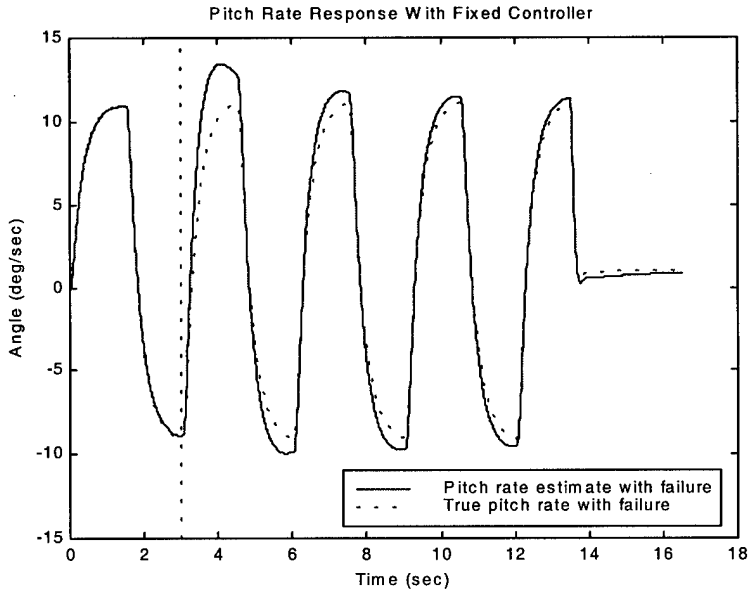

Figure 9. Pitch rate response with a fixed controller; $\sigma_\alpha = 0.03$ deg/sec, K=0.8, SNR=18.61 dB.

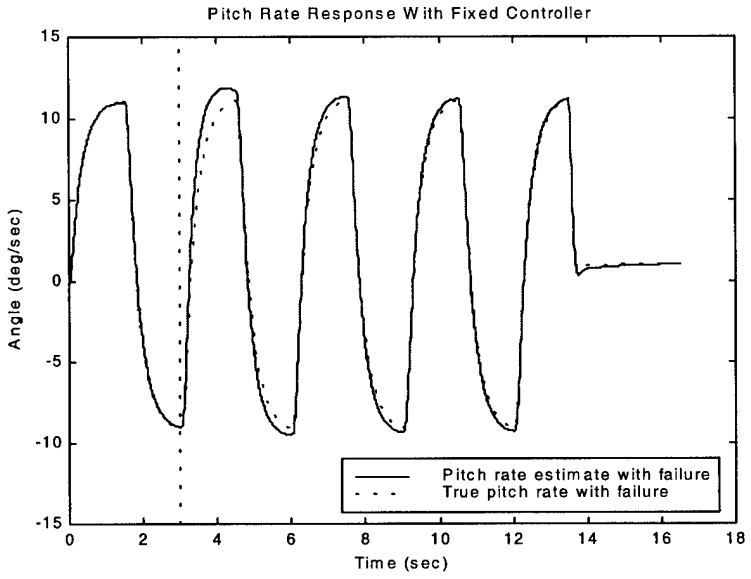

Figure 10. Pitch rate response with a fixed controller; $\sigma_\alpha = 0.3$ deg/sec, K=0.8, SNR=18.61 dB.

The noise vector used in this thesis was created using the Matlab® RANDN(N) function [12]. This command picks data points from a normal distribution with mean zero and variance equal to one. After every run of the simulation code, the noise generator is reset to a initial point inside Matlab®. This created a fixed single noise sample for all simulations. A better method would have been to set up a Monte Carlo run, generating hundreds of noise vectors and averaging them to get more random noise input. However, running a Monte Carlo analysis is time consuming and is not a necessary focus for this thesis.

Process noise is represented in the system identification algorithm as w,however, no process noise is implemented in the simulation runs. This is done to show that the estimation techniques described in this thesis work in a deterministic case. The only noise used in the simulations are the alpha and pitch rate channel measurement noise needed for the algorithm.

1.5 Organization of Thesis

Chapter 1 provided an overview of the problem statement, a description of the proposed plant and the assumptions and reasoning for various parts of the research. Chapter 2 gives the classical approach to system identification, an example of a second order system and a stochastic approach when noise is introduced into the system. Chapter 3 introduces the deterministic approach to the system ID algorithm used in the thesis. The stochastic approach to the algorithm presented in Chapter 4 will be the main system identification algorithm. Chapter 4 also provides examples and remarks concerning the development of the open-loop gain system identification algorithm. A numerical simulation experiment is performed. Thus, a flight control experiment is performed and numerical simulation results which corroborate the developed theory are presented Chapter 5. The effects of sensor noise on identification performance are also investigated and presented in Chapter 5. Concluding remarks are made is Chapter 6.

Chapter 2 - System Identification

2.1 Introduction

This chapter provides general background knowledge of system identification techniques. Both the classical and stochastic analysis methods are explained and examples are given. Also, some concerns and design considerations related to system identification are addressed.

When modeling a system, there are two approaches of consideration, deductive and empirical [17]. With deductive modeling, the laws and equations found in physics and engineering are used to predict the proper model. With the empirical (system identification) approach, least squares and Kalman estimates are found to form a statistical approach for determining a dynamics of the system.

System identification has more applications than just for modeling purposes. It is also a useful technique for model order reduction of a plant or compensator, for measuring or estimating parameters and for real time adaptive control.

One of the challenges that needs to be addressed is modeling error, especially when the order of the system, n, is not known. This error may consist of various disturbances such as process and measurement noises. Over-modeling is another source of error in system identification. It may seem logical to over-model a system. The extra parameters would be redundant and make determining the over-all system model easier. When determining the unknown parameters of a higher order model, the parameters that exceed the order of the physical system should equal zero and fall out of the equation. However, this does not always happen because of rounding, noise and other anomalies being injected into the calculations. These approximated values disturb the pole and zero placements of the system. Therefore, it is better to under-estimate the order of the unknown system than to over-estimate it. Under-modeling requires determining values for the parameters, $a_1, a_2, \cdots, b_1, b_2, \cdots$, that yield the best fit over a desired bandwidth.

2.2 Classical System Identification

Consider the continuous-time transfer function (TF) [17]

$$H(s) = \frac{y(s)}{u(s)} = \frac{b_1 s^{n-1} + b_2 s^{n-2} + \cdots + b_{n-1}s + b_n}{s^n - a_1 s^{n-1} - a_2 s^{n-2} - \cdots - a_{n-1}s - a_n} \tag{7}$$

If we chose the input to be

$$u_k(t) = \sin \omega_k t, \quad 0 \leq t \tag{8}$$

The output is the phasor

$$\begin{aligned} y_k(t) &= (A_k + jB_k)\sin\omega_k t \\ &= \sqrt{A_k^2 + B_k^2}\sin(\omega_k t + \phi) \\ &= A\sin(\omega_k t + \phi) \end{aligned} \tag{9}$$

where

$$\phi = A\tan\left(\frac{B_k}{A_k}\right) \tag{10}$$

Letting $s = j\omega$ and substituting into H(s)

$$\begin{aligned} H(s) &= \frac{y(s)}{u(s)} = A_k + jB_k \\ &= \frac{b_1(j\omega_k)^{n-1} + b_2(j\omega_k)^{n-2} + \cdots + b_{n-1}(j\omega_k) + b_n}{(j\omega_k)^n - a_1(j\omega_k)^{n-1} - a_2(j\omega_k)^{n-2} - \cdots - a_{n-1}(j\omega_k) - a_n} \end{aligned} \tag{11}$$

Cross multiplying and reducing creates a linear equation where the coefficients a and b can be obtained.

$$A_k + jB_k = \sum_{i=1}^{n}(A_k + jB_k)(j\omega_k)^{-i}a_i + \sum_{i=1}^{n}(j\omega_k)^{-i}b_i \tag{12}$$

Expanding the equation gives

$$\begin{aligned} A_k + jB_k &= \frac{1}{j}(A_k + jB_k)(\frac{1}{\omega_k}a_1 - \frac{1}{\omega_k^3}a_3 + \frac{1}{\omega_k^5}a_5 - \frac{1}{\omega_k^7}a^7 + \cdots) \\ &\quad + \frac{1}{j}(\frac{1}{\omega_k}b_1 - \frac{1}{\omega_k^3}b_3 + \frac{1}{\omega_k^5}b_5 - \frac{1}{\omega_k^7}b^7 + \cdots) \\ &\quad + (A_k + jB_k)(-\frac{1}{\omega_{k^2}}a_2 + \frac{1}{\omega_k^4}a_4 - \frac{1}{\omega_k^6}a_6 + \cdots) \\ &\quad + (-\frac{1}{\omega_{k^2}}b_2 + \frac{1}{\omega_k^4}b_4 - \frac{1}{\omega_k^6}b_6 + \cdots) \end{aligned} \tag{13}$$

Multiplying both sides by j and expanding, we are able to match the real and complex portions of the right side of the equation with the left. This will allow us to solve for the unknown coefficients.

$$\begin{aligned} -B_k &= A_k(\frac{1}{\omega_k}a_1 - \frac{1}{\omega_k^3}a_3 + \frac{1}{\omega_k^5}a_5 - \frac{1}{\omega_k^7}a^7 + \cdots) \\ &\quad +B_k(\frac{1}{\omega_{k^2}}a_2 - \frac{1}{\omega_k^4}a_4 + \frac{1}{\omega_k^6}a_6 - \cdots) \\ &\quad +(\frac{1}{\omega_k}b_1 - \frac{1}{\omega_k^3}b_3 + \frac{1}{\omega_k^5}b_5 - \frac{1}{\omega_k^7}b^7 + \cdots) \end{aligned}$$

$$\begin{aligned} A_k &= B_k(\frac{1}{\omega_k}a_1 - \frac{1}{\omega_k^3}a_3 + \frac{1}{\omega_k^5}a_5 - \frac{1}{\omega_k^7}a^7 + \cdots) \\ &\quad +A_k(-\frac{1}{\omega_{k^2}}a_2 + \frac{1}{\omega_k^4}a_4 - \frac{1}{\omega_k^6}a_6 + \cdots) \\ &\quad +(-\frac{1}{\omega_{k^2}}b_2 + \frac{1}{\omega_k^4}b_4 - \frac{1}{\omega_k^6}b_6 + \cdots) \end{aligned} \tag{14}$$

For an n^{th} order SISO system, the control system is specified by 2n parameters. For this reason, we chose n sinusoidal test functions, each one producing 2n equations.

2.2.1 Second Order Example

Given the TF [17]

$$H(s) = \frac{\omega_n^2}{s^2 + 2\zeta\omega_n s + \omega_n^2}$$

Knowing that we can measure the output phasor, the unknown parameters, δ and ω_n, can be solved using the technique described in Eqs. (11)-(14):

$$A + jB = \frac{\omega_n^2}{-\omega^2 + 2\zeta\omega_n j\omega + \omega_n^2}$$

Cross multiplying and simplifying yields

$$(A + jB)(\omega_n^2 - \omega^2 + 2\zeta\omega_n j\omega) = \omega_n^2$$

$\Longrightarrow$

$$(A-1)\omega_n^2 - 2B\omega(\zeta\omega_n) - A\omega^2 + j(B\omega_n^2 + 2A\omega(\zeta\omega) - B\omega^2) = 0$$

Separating the complex and real terms

$$\begin{aligned}(A-1)\omega_n^2 - 2B\omega(\zeta\omega_n) &= A\omega^2 \\ B\omega_n^2 + 2A\omega(\zeta\omega) &= B\omega^2\end{aligned}$$

Solving for natural frequency and damping ratio, the unknown parameters, yields

$$\begin{aligned}\omega_n &= \sqrt{\frac{A^2+B^2}{A^2+B^2-A}}\omega \\ \zeta &= -\frac{B}{2\sqrt{(A^2+B^2-A)(A^2+B^2)}}\end{aligned}$$

Recall, A and B are the coefficients of the output phasor and can be directly measured.

2.3 Stochastic Analysis

A goal of system identification is to find a "best fit" model of the system being analyzed [15]. The stochastic analysis takes the measurable input and output data, which has some noise influence. Using a least-squares approach, the sum of the squared errors between the true output of the model and the measured output is minimized. Using the least-squares approach and stochastic estimation, large errors and poor measurements are given less value or priority than more accurate measurements. Because of the introduction of noise into the system and consequently the implementation of stochastic analysis, our once continuous system is now discretized and represented as a discrete-time model.

In a case of a dynamic system, a system output can be described as [7, 15, 17]

$$y_{k+1} = a_1 y_k + a_2 y_{k-1} + \cdots + a_n y_{k-n+1} + b_1 u_k + b_2 u_{k-1} + \cdots + b_m u_{k-m+1} \tag{15}$$

and the measurement equation as

$$z_{k+1} = y_{k+1} + v_{k+1}, \quad v_{k+1} = N(0, \sigma^2) \tag{16}$$

which may contain process and disturbance noise. Manipulating the above equation a little we can say

$$y_{k+1} = z_{k+1} - v_{k+1}$$

$$y_k = z_k - v_k$$

Therefore,

$$\begin{aligned} z_{k+1} - v_{k+1} &= a_1(z_k - v_k) + a_2(z_{k+1} - v_{k-1}) + \cdots + a_n(z_{k-n+1} - v_{k-n+1}) \\ &\quad + b_1 u_k + b_2 u_{k-1} + \cdots + b_m u_{k-m+1} \end{aligned} \tag{17}$$

By defining a noise vector, $\tilde{\mathrm{V}}_{k+1}$, we can rearrange the above equation

$$\begin{aligned} z_{k+1} &= a_1 z_k + a_2 z_{k-1} + \cdots + a_n z_{k-n+1} + b_1 u_k + b_2 u_{k-1} + \cdots + b_m u_{k-m+1} \\ &\quad + \tilde{V}_{k+1} \end{aligned}$$

where

$$\tilde{V}_{k+1} \triangleq v_{k+1} - a_1 v_k - a_2 v_{k-1} + \cdots - a_n v_{k-n+1} \tag{18}$$

Now, the measurement equation is defined as

$$Z = H\Theta + \tilde{V} \tag{19}$$

where

$$Z \triangleq \begin{pmatrix} z_{k+1} \\ z_{k+2} \\ \vdots \\ z_{k+N+1} \end{pmatrix}_{(N+1)\times 1}, \quad \Theta \triangleq \begin{pmatrix} a_1 \\ \vdots \\ a_n \\ b_1 \\ \vdots \\ b_m \end{pmatrix}_{(m+n)\times 1}, \quad \tilde{V} \triangleq \begin{pmatrix} \tilde{V}_{k+1} \\ \tilde{V}_{k+2} \\ \vdots \\ \tilde{V}_{k+N+1} \end{pmatrix}_{(N+1)\times 1} \tag{20}$$

and

$$H \triangleq \begin{pmatrix} z_k & z_{k-1} & \cdots & z_{k-n+1} & u_k & u_{k-1} & \cdots & u_{k-m+1} \\ z_{k+1} & z_k & \cdots & z_{k-n+2} & u_{k+1} & u_k & \cdots & u_{k-m+2} \\ \vdots & \vdots & & \vdots & \vdots & \vdots & & \vdots \\ z_{k+N} & z_{k+N-1} & \cdots & z_{k+N-n+1} & u_{k+N} & u_{k+N-1} & \cdots & u_{k-m+N} \end{pmatrix}_{(N+1)\times(m+n)} \tag{21}$$

In this notation, m is the number of measurements and n is the number of parameters to be identified. We can now find the Least Squares estimate, $\hat{\Theta}$, and the error covariance matrix P [1, 17].

The Least Squares estimate is defined as

$$\hat{\Theta} = (H^T H)^{-1} H^T Z \tag{22}$$

The above equation calculates the parameter estimates using an unweighted pseudo-inverse. This is possible when the weighting matrix, R, is assumed to be diagonal or when cross correlation does not exist. When this assumption is made, $R = \sigma^2 I$, where I is the identity matrix and σ^2 the strength of the noise, drops out of the equation.

The error covariance is defined as

$$P = \sigma^2 (H^T H)^{-1} \tag{23}$$

It too does not take into effect the measurement or process noise when estimating the parameters. A more rigorous method would be to solve for the parameter estimates and error using a weighted pseudo-inverse to account for any noise in the system. The minimum-variance estimate is defined as [3, 4]

$$\hat{\Theta}_{MV} = (H^T R^{-1} H)^{-1} H^T R^{-1} Z \tag{24}$$

and the minimum-error-estimate is

$$P_{mv} = \sigma^2 (H^T R^{-1} H)^{-1} \tag{25}$$

2.4 Calculating R

R is affected by the noise created by our sensors when measuring the output of the system. Many times, R is represented as a diagonal matrix with σ^2 along the diagonal and zeros in the off-diagonal spaces which represents no cross correlation. This seems true knowing each output has its own independent sensor to take measurements. In truth, the sensors are coupled to some extent [17]. This causes off-diagonal terms in the R matrix. Before we described R as being the expected value of the measurement noise times the transpose of that noise. It is shown from Eq. (20) that

the measurement noise is actually a noise vector, $\tilde{V}$. This noise vector now produces off-diagonal terms in the R matrix.

R, using a two parameter example, is now defined as

$$
\begin{aligned}
R &= E(\tilde{V}\tilde{V}^T) = E\left(\begin{pmatrix} \tilde{V}_{k+1} \\ \vdots \\ \tilde{V}_{k+N} \end{pmatrix} \begin{pmatrix} \tilde{V}_{k+1} & \cdots & \tilde{V}_{k+N} \end{pmatrix}\right) \\
&= E\left(\begin{pmatrix} v_{k+1} - a_1 v_k \\ v_{k+2} - a_1 v_{k+1} \\ \vdots \\ v_{k+N} - a_1 v_{k+N-1} \end{pmatrix} \begin{pmatrix} v_{k+1} - a_1 v_k & v_{k+2} - a_1 v_{k+1} & \cdots & v_{k+N} - a_1 v_{k+N-1} \end{pmatrix}\right) \\
&= E\begin{pmatrix} (v_{k+1} - a_1 v_k)(v_{k+1} - a_1 v_k) & (v_{k+1} - a_1 v_k)(v_{k+2} - a_1 v_{k+1}) & \cdots \\ (v_{k+2} - a_1 v_{k+1})(v_{k+1} - a_1 v_k) & (v_{k+2} - a_1 v_{k+1})(v_{k+2} - a_1 v_{k+1}) & \cdots \\ \vdots & \vdots & \end{pmatrix} \\
&= \begin{pmatrix} \sigma^2 + a^2\sigma^2 & -a\sigma^2 & 0 & 0 & \cdots \\ -a\sigma^2 & \sigma^2 + a^2\sigma^2 & -a\sigma^2 & 0 & \cdots \\ 0 & -a\sigma^2 & \sigma^2 + a^2\sigma^2 & -a\sigma^2 & 0 \\ 0 & 0 & -a\sigma^2 & \sigma^2 + a^2\sigma^2 & \ddots \\ \vdots & \vdots & 0 & -a\sigma^2 & \ddots \end{pmatrix}
\end{aligned} \tag{26}
$$

Finally,

$$
R = \sigma^2 \begin{pmatrix} 1 + a^2 & -a & 0 & \\ -a & 1 + a^2 & -a & \ddots \\ 0 & -a & \ddots & \ddots \\ & \ddots & \ddots & \ddots \end{pmatrix}
$$

In summary, the parameters of an unknown plant can be identified by using a sinusoidal test function as an input to that unknown plant and observing the phasor output. However, care must be taken not to over-model the unknown plant. When noise is included in the system dynamcis, stochastic analysis must be used to account for the effects. A discrete-time model was given and the input and measurement equations, now with a noise term, were defined . It was then shown how the strength of the noise can be represented as a weighting matrix, R, and applied to the state estimates to provide more accurate results.

Chapter 3 - Deterministic Model

A physical system can be adequately represented as a mathematical model in order to investigate its dynamic characteristics and system responses. Sensors are used to measure the states required for the control law. The control law is simply the feedback of all the states required in the system identification algorithm [9]. It will be discussed further in Chapter 5. Although the proposed plant involves using a stochastic model to generate the state estimates, as in Fig. 1, it is necessary to create a deterministic model first. The deterministic model is the simplest model. With a deterministic model, physical noise is not introduced into the system. By removing the noise, the model and mathematics are made simpler. This allows us to see the true relationship between the input command and the output responses. It also helps the designer determine if a compensator is needed to improve system performance. The desired state parameters must be able to be calculated deterministically if one hopes to observe them later when noise is an influence.

3.1 Deterministic Model Setup

The aircraft model is an F-16 class aircraft flying at Mach 0.9 at 20,000 feet and the (unstable) short period pitch dynamics approximation is used [16]. The relevant states are α and q, the aircraft angle of attack and pitch rate, respectively, and the control variable is the elevator deflection δ_e. The plant truth model used in the system identification algorithm is

$$\begin{aligned} \dot{\alpha} &= Z_\alpha \alpha + Z_q q + K Z_{\delta_e} \\ \dot{q} &= M_\alpha \alpha + M_q q + K M_{\delta_e} \end{aligned}$$

The Z derivatives are

$$Z_\alpha = -1.3433, \quad Z_q = 0.9946, \quad Z_{\delta e} = -0.1525$$

and the M derivatives are

$$M_\alpha = 3.5, \quad M_q = -1.0521, \quad M_{\delta e} = -24.3282$$

In continuous state space form, the bare aircraft (plant) dynamics are

$$\begin{aligned}\dot{x} &= Ax + bu \\ &= \begin{pmatrix} -1.3433 & 0.9946 \\ 1.2915 & -1.0521 \end{pmatrix} x + \begin{pmatrix} -0.1525 \\ -24.3282 \end{pmatrix} u\end{aligned}$$

where the states

$$x = \begin{pmatrix} \alpha \\ q \end{pmatrix}$$

evolve in $\Re^2$ and u is the elevator deflection δ_e.

The input is three pitch rate doublet commands (q command), having an amplitude of ± 10 degrees and a period of 4.5 seconds giving a 13.5 second record. The doublets are passed through a low pass filter, $\frac{3}{S+3}$, and applied to a unit step to give a 13.5 second period of excitation and 3 seconds of steady control for a combined 16.5 seconds of data. The input command represents a pilot "exciting the stick"or applying dynamic movement to the aircraft's elevator.

The input command is then summed with the states α and q using state feedback. The elevator command then goes through a first order actuator with a bandwidth of 20.0 rad/sec, $\frac{20}{S+20}$. This signal, δ_e, is the input signal into the plant.

Augmenting the A and b matrix with the actuator dynamics yields

$$\begin{aligned}\dot{x} &= A\,x + b\,u \\ &= \begin{pmatrix} Z_\alpha & Z_q & Z_{\delta_e} \\ M_\alpha & M_q & M_{\delta_e} \\ 0 & 0 & -\frac{1}{\tau} \end{pmatrix} x + \begin{pmatrix} 0 \\ 0 \\ \frac{1}{\tau} \end{pmatrix} \delta_{e_c}\end{aligned}$$

where the states are now

$$x = \begin{pmatrix} \alpha \\ q \\ \delta_e \end{pmatrix}$$

and the control input is δ_{e_c}.

$$\delta_{e_c} = r - (K_\alpha + K_q + K_{\delta_e})x$$

and the actuator dynamics are

$$\dot{\delta}_e = -\frac{1}{\tau}\delta_e + \frac{1}{\tau}\delta_{e_c}$$

where $\tau = 0.05\,\text{sec}$.

The closed loop A matrix is now formed using state feedback. The resulting A and b closed loop matrices are

$$\begin{aligned} A_{cl} &= A + b\begin{bmatrix} K_\alpha & -K_q & -K_{\delta_e} \end{bmatrix} \\ &= \left(\begin{pmatrix} Z_\alpha & Z_q & Z_{\delta e} \\ M_\alpha & M_q & M_{\delta e} \\ 0 & 0 & -\frac{1}{\tau} \end{pmatrix} + \begin{pmatrix} 0 \\ 0 \\ \frac{1}{\tau} \end{pmatrix} \begin{bmatrix} -K_\alpha & -K_q & -K_{\delta_e} \end{bmatrix} \right) \\ &= \begin{pmatrix} Z_\alpha & Z_q & Z_{\delta e} \\ M_\alpha & M_q & M_{\delta e} \\ -\frac{1}{\tau}K_\alpha & -\frac{1}{\tau}K_q & -\frac{1}{\tau}(1+K_{\delta_e}) \end{pmatrix} \end{aligned}$$

$$B_{cl} = \begin{pmatrix} 0 \\ 0 \\ \frac{1}{\tau} \end{pmatrix}$$

so we get

$$\dot{x} = A_{cl}\, x + b_{cl} u$$

The system as is will not track a step input, so a proportional or a PI controller can be included to adjust the tracking.

3.2 Proportional Controller

To find the gain needed to improve tracking performance, the augmented closed-loop state space equation is used. The reference signal r ($\equiv q$) is the exogenous input and $\delta_c = K_r r - K_\alpha \alpha - K_q q - K_{\delta_e}$. At steady state, $\dot{x} = A_{cl}\, x + b K_r r = 0$. Writing the augmented state space equation with the necessary gain, K_r, at steady state

$$0 = A_{cl}\, \bar{x} + K_r b r$$

and solving for $\bar{x}$ yields

$$\bar{x} = K_r A_{cl}^{-1} b r$$

Substituting the above into the output equation

$$\bar{y} = c\bar{x}$$

gives us

$$\bar{y} = K_r c(A_{cl}^{-1} br)$$

It is desired for the output to track a step input. For this to happen $\bar{y} = r \Longrightarrow$

$$1 = K_r c A_{cl}^{-1} b$$

must hold. Solving for K_r, yields

$$K_r = \frac{1}{cAcl^{-1}b}$$

which gives the required gain needed for proper tracking. This gain is then applied to the system before the feedback loop as shown in Fig. 1, Chapter 1. This adjusts our B_{cl} to the following

$$B_{cl} = \begin{pmatrix} 0 \\ 0 \\ \frac{K_r}{\tau} \end{pmatrix}$$

The gains needed for K_α, $K_q$and K_{δ_e} are

$$K_\alpha = 0.283$$

$$K_q = 0.876$$

$$K_{\delta_e} = 0.3$$

3.3 PI Controller

Because the tracking error, or steady state error, is large but the transient response is adequate, a PI controller can be used [8]. It works by increasing the system type without significantly changing the dominant roots of the characteristic equation. This is done by placing a zero close to the origin to counteract the integrator pole located at the origin. This way, the system response is maintained very close to the original and the tracking error is reduced.

Using a PI controller to obtain tracking causes the A and b matrices to change because of the additional integrator state.

$$\dot{x} = \begin{pmatrix} Z_\alpha & Z_q & Z_{\delta e} & 0 \\ M_\alpha & M_q & M_{\delta e} & 0 \\ 0 & 0 & -\frac{1}{\tau} & 0 \\ 0 & -1 & 0 & 0 \end{pmatrix} x + \begin{pmatrix} 0 \\ 0 \\ 0 \\ 1 \end{pmatrix} r + \begin{pmatrix} 0 \\ 0 \\ \frac{1}{\tau} \\ 0 \end{pmatrix} \delta_c$$

where the states are now

$$x = \begin{pmatrix} \alpha \\ q \\ \delta_e \\ z \end{pmatrix}$$

and r is the reference signal. Now,

$$\begin{aligned} \delta_c &= r - -K_\alpha \alpha - K_q q - K_{\delta_e} \delta_e + K_z z \\ \dot{z} &= r - q \end{aligned}$$

The new A_{cl} and B_{cl} matrices are

$$\begin{aligned} A_{cl} &= A + b \begin{bmatrix} -K_\alpha & -K_q & -K_{\delta_e} & K_z \end{bmatrix} \\ &= \begin{pmatrix} Z_\alpha & Z_q & Z_{\delta e} & 0 \\ M_\alpha & M_q & M_{\delta e} & 0 \\ \frac{K_\alpha}{\tau} & \frac{K_q}{\tau} & -\frac{(1+K_{\delta_e})}{\tau} & \frac{K_z}{\tau} \\ 0 & -1 & 0 & 0 \end{pmatrix} \end{aligned}$$

$$Bcl = \begin{pmatrix} 0 \\ 0 \\ \frac{1}{\tau} \\ 1 \end{pmatrix}$$

The gains needed to improve tracking performance are

$$\begin{aligned} K_a &= 0.283 \\ K_q &= 0.876 \\ K_{\delta_e} &= -0.4 \\ K_z &= -0.0001 \end{aligned}$$

In this chapter, the deterministic model of the thesis problem was addressed. It was shown how the actuator dynamics was augmented with the A and b matrix, and the control law defined. Because the control system could not properly track a step input, a proportional and a PI controller were implemented for two different case studies. The closed loop matrices were found for both fixed controllers and the gains identified.

Chapter 4 - Stochastic Model

A deterministic system may not always provide a complete and a sufficient method for data analysis. There are three basic reasons why this may be so [13].

As said before, a physical system can be adequately represented as a mathematical model. While this is true, it also says that no model is a perfect model. The model may be sufficient enough to observe those responses the designer finds important but many physical systems are very complex and nonlinear. Nonlinear systems are often linearized about some nominal point and the higher order terms are often neglected to make algorithms simpler and reduce computer processing time. Therefore, mathematical models are designed with error and uncertainty in it.

Dynamic systems, such as an aircraft, are not just controlled by the user. Many external sources also serve as inputs into the system. These disturbances can come from wind, moisture, computer and actuator system delays. In short, most systems cannot be represented as a single input system. Factors are always present that can't be modeled in a deterministic system.

Just as mathematical models are not perfect models, sensors, or measurement devices, are not perfect either. When states are measured using a device external to the model, imperfections are introduced. Therefore, the measurements displayed by the sensor are corrupted by its own design imperfections, system responses and noise. Another problem with sensors is that not all system variables are able to be measured with a common sensor device. For these situations, and for the reasons above, a stochastic estimation model is used.

A stochastic system model is created with the help of a Kalman filter. A Kalman filter is basically a data processing algorithm that uses all available data, such as initial conditions, plant model, and statistical descriptions of any biases, noise or model uncertainty. This information is

fed into the propagate/update algorithm which then optimally derives an estimated value for the system states or any other variables of interest in a way that minimizes error.

4.1 Recursive System Identification Algorithm

The novel loop gain system identification algorithm is stated in Theorem 1. Since measurement noise is now being introduced into the system, a discrete-time model is used.

Theorem 1 *Consider the following linear estimation problem. The linear dynamical system is*

$$x_{k+1} = Ax_k + Kbu_k + \Gamma w_k, \quad k = 0, 1, ..., N-1, \quad E(w_k w_k^T) = Q \tag{27a}$$

The prior information is

$$x_o = N(\bar{x}_o, P_{o_x}) \tag{28a}$$

$$K = N(K_o, P_{o_K}) \tag{28b}$$

The output signal

$$y_{k+1} = Cx_{k+1} \tag{29}$$

and the observation equation is

$$z_{k+1} = y_{k+1} + v_{k+1}, \quad E(v_{k+1} v_{k+1}^T) = R. \tag{30a}$$

The martices A, b, C and Γ are known. The respective process noise and measurement noise covariance matrices, Q and R, are also known.

Denote by $\hat{x}_k$ and $\hat{K}_k$ the respective estimates of the state at time k, x_k and the loop gain K, given the measurements record $z_1, ...z_k$, the input sequence $u_0, ..., u_{k-1}$, and the prior information on x_o and K. The covariance of the estimation error of the $\begin{pmatrix} x_k \\ K \end{pmatrix}$ vector is denoted by the partitioned matrix $P_k = \begin{pmatrix} P_{k_{xx}} & p_{k_{xK}} \\ p_{k_{xK}}^T & p_{k_{KK}} \end{pmatrix}$,

Initially, set

$$\hat{x}_o \triangleq \bar{x}_o, \qquad \hat{K}_o \triangleq K_o, \qquad P_{o_{xx}} \triangleq P_{o_x}, \qquad p_{o_{KK}} \triangleq P_{o_K}, \qquad p_{o_{xK}} \triangleq 0.$$

Then for $k = 0, 1, ..., N-1$, the state and gain estimates are

$$\hat{x}_{k+1} = A\hat{x}_k + \hat{K}_k bu_k + K_x(z_{k+1} - CA\hat{x}_k - \hat{K}_k Cbu_k) \tag{31}$$

$$\hat{K}_{k+1} = \hat{K}_k + K_K(z_{k+1} - CA\hat{x}_k - \hat{K}_k Cbu_k) \tag{32}$$

where the Kalman gains

$$\begin{aligned} K_x = {} & \{AP_{k_{xx}}A^TC^T + u_k[Ap_{k_{xK}}(Cb)^T + b(CAp_{k_{xK}})^T] \\ & + u_k^2 p_{k_{KK}} b(Cb)^T + \Gamma Q \Gamma^T C^T\} \times \{CAP_{k_{xx}}A^TC^T \\ & + u_k[CAp_{k_{xK}}(Cb)^T + (Cb)(CAp_{k_{xK}})^T] \\ & + u_k^2 p_{k_{KK}}(Cb)(Cb)^T + C\Gamma Q\Gamma^T C^T + R\}^{-1} \end{aligned} \tag{33a}$$

and

$$\begin{aligned} K_K = {} & [(CAp_{k_{xK}})^T + u_k p_{k_{KK}}(Cb)^T] \times \{CAP_{k_{xx}}A^TC^T \\ & + u_k[CAp_{k_{xK}}(Cb)^T + (Cb)(CAp_{k_{xK}})^T] \\ & + u_k^2 p_{k_{KK}}(Cb)(Cb)^T + C\Gamma Q\Gamma^T C^T + R\}^{-1} \end{aligned} \tag{34}$$

Furthermore, the estimation error covariances are

$$\begin{aligned} P_{k+1_{xx}} &= \{[AP_{k_{xx}}A^T + u_k(Ap_{k_{xK}}b^T + bp_{k_{xK}}^T A^T) \\ &\quad + u_k p_{k_{KK}} bb^T + \Gamma Q \Gamma^T]^{-1} + C^T R^{-1} C\}^{-1} \end{aligned} \tag{35}$$

$$\begin{aligned} p_{k+1_{KK}} &= p_{k_{KK}} - [(CAp_{k_{xK}})^T + u_k p_{k_{KK}}(Cb)^T]\{CAP_{k_{xx}}A^T C^T \\ &\quad + u_k[CAp_{k_{xK}}(Cb)^T + (Cb)(CAp_{k_{xK}})^T] + u_k^2 p_{k_{KK}}(Cb)(Cb)^T \\ &\quad + C\Gamma Q \Gamma^T C^T + R\}^{-1}(CAp_{k_{xK}} + u_k p_{k_{KK}}(Cb)) \end{aligned} \tag{36}$$

$$\begin{aligned} p_{k+1_{xK}} &= Ap_{k_{xK}} + u_k p_{k_{KK}} b - \{AP_{k_{xx}}A^T C^T + u_k[Ap_{k_{xK}}(Cb)^T \\ &\quad + b(CAp_{k_{xK}})^T] + u_k^2 p_{k_{KK}} b(Cb)^T + \Gamma Q \Gamma^T C^T\} \times \\ &\quad \{CAP_{k_{xx}}A^T C^T + u_k[CAp_{k_{xK}}(Cb)^T + (Cb)(CAp_{k_{xK}})^T] \\ &\quad + u_k^2 p_{k_{KK}}(Cb)(Cb)^T + C\Gamma Q \Gamma^T C^T + R\}^{-1} \times \\ &\quad (CAp_{k_{xK}} + u_k p_{k_{KK}}(Cb)) \end{aligned} \tag{37}$$

4.2 Proof of Theorem

The proof of Theorem 1 is given below:

Since the unknown loop gain K is a constant, we augment the dynamics as follows.

$$K_{k+1} = K_k \tag{38}$$

Hence, the augmented state dynamics evolve in $\Re^{n+1}$and are

$$\begin{pmatrix} x_{k+1} \\ K_{k+1} \end{pmatrix} = \begin{pmatrix} A & u_k b \\ 0 & 1 \end{pmatrix} \begin{pmatrix} x_k \\ K_k \end{pmatrix} + \begin{pmatrix} \Gamma \\ 0 \end{pmatrix} w_k \tag{39}$$

and the measurement equation is

$$z_{k+1} = \begin{pmatrix} C & \vdots & 0 \end{pmatrix} \begin{pmatrix} x_{k+1} \\ K_{k+1} \end{pmatrix} + v_{k+1} \tag{40}$$

As you can see, the equations are similar to that of the deterministic model except for noise now being modeled into the system. Here, the w_k and v_{k+1} represent the process noise and measurement noise respectively. The covariances of these noises are represented as Q and R in the stochastic model. The values of Q and R were defined in Chapter 1.

The prior information at time k is

$$\begin{pmatrix} x_k \\ K_k \end{pmatrix} = N\left(\begin{pmatrix} \hat{x}_k \\ \hat{K}_k \end{pmatrix}, P_{k_{(x,K)}}\right) \tag{41}$$

where

$$P_{k_{(x,K)}} = \begin{pmatrix} P_{k_{xx}} & p_{k_{xK}} \\ p_{k_{xK}}^T & p_{k_{KK}} \end{pmatrix} \tag{42}$$

is the estimation error covariance matrix.

Note: The estimation error covariance matrix is partitioned as follows,

$$P_{k_{xx}} \in \Re^{n \times n}, \quad p_{k_{xK}} \in \Re^{n}, \quad p_{k_{KK}} \in \Re^{1} \tag{43}$$

Hence, before the z_{k+1} measurement is recorded, the augmented state

$$\begin{pmatrix} x_{k+1} \\ K_{k+1} \end{pmatrix} = N\left(\begin{pmatrix} A & u_k b \\ 0 & 1 \end{pmatrix}\begin{pmatrix} \hat{x}_k \\ \hat{K}_k \end{pmatrix}, \begin{pmatrix} A & u_k b \\ 0 & 1 \end{pmatrix} P_{k_{(x,K)}} \begin{pmatrix} A^T & 0 \\ u_k b^T & 1 \end{pmatrix} + \begin{pmatrix} \Gamma Q \Gamma^T & 0 \\ 0 & 0 \end{pmatrix}\right)$$

$$= N\left(\begin{pmatrix} A\hat{x}_k + \hat{K}_k b u_k \\ \hat{K}_k \end{pmatrix}, \begin{pmatrix} AP_{k_{xx}}A^T + u_k(AP_{k_{xK}}b^T + bp_{k_{xK}}^T A^T) + u_k^2 p_{k_{KK}} bb^T + \Gamma Q \Gamma^T & \vdots & Ap_{k_{xK}} + u_k p_{k_{KK}} b \\ \cdots\cdots\cdots\cdots & \vdots & \cdots\cdots\cdots \\ p_{k_{xK}}^T A^T + u_k p_{k_{KK}} b^T & \vdots & p_{k_{KK}} \end{pmatrix}\right)$$

Next, apply the Bayesian estimation formula

$$\hat{x}^+ = \hat{x}^- + K\left[z - H\hat{x}\right],$$

viz.,

$$\begin{pmatrix} \hat{x}_{k+1} \\ \hat{K}_{k+1} \end{pmatrix} = \begin{pmatrix} A\hat{x}_k + \hat{K}_k b u_k \\ \hat{K}_k \end{pmatrix} + K\left(z_{k+1} - \begin{pmatrix} C & \vdots & 0 \end{pmatrix}\begin{pmatrix} A\hat{x}_k + \hat{K}_k b u_k \\ \hat{K}_k \end{pmatrix}\right)$$

$$= \begin{pmatrix} A\hat{x}_k + \hat{K}_k b u_k \\ \hat{K}_k \end{pmatrix} + K\left(z_{k+1} - CA\hat{x}_k - u_k \hat{K}_k C b\right)$$

where the Kalman gain

$$
\begin{aligned}
K &= \begin{pmatrix} AP_{k_{xx}}A^T + u_k(Ap_{k_{xK}}b^T + bp_{k_{xK}}^T A^T) & \vdots & Ap_{k_{xK}} + u_k p_{k_{KK}} b \\ +u_k^2 p_{k_{KK}} bb^T + \Gamma Q \Gamma^T & \vdots & \\ \cdots\cdots\cdots\cdots\cdots\cdots\cdots\cdots\cdots\cdots & \vdots & \cdots\cdots\cdots\cdots \\ p_{k_{xK}}^T A^T + u_k p_{k_{KK}} b^T & \vdots & p_{k_{KK}} \end{pmatrix} \\
& \begin{pmatrix} C^T \\ 0 \end{pmatrix} \times \{CAP_{k_{xx}}A^T C^T + u_k[CAp_{k_{xK}}(Cb)^T + (Cb)(CAp_{k_{xK}})^T] \\
& + u_k^2 p_{k_{KK}}(Cb)(Cb)^T + C\Gamma Q \Gamma^T C^T + R\}^{-1} \\
&= \begin{pmatrix} AP_{k_{xx}}A^T C^T + u_k[Ap_{k_{xK}}(Cb)^T + b(CAp_{k_{xK}})^T] \\ +u_k^2 p_{k_{KK}} b(Cb)^T + \Gamma Q \Gamma^T C^T \\ \cdots\cdots\cdots\cdots\cdots\cdots\cdots\cdots\cdots\cdots\cdots\cdots\cdots\cdots\cdots\cdots \\ (CAp_{k_{xK}})^T + u_k p_{k_{KK}}(Cb)^T \end{pmatrix} \times \\
& \{CAP_{k_{xx}}A^T C^T + u_k[CAp_{k_{xK}}(Cb)^T + Cb(CAp_{k_{xK}})^T] \\
& + u_k^2 p_{k_{KK}}(Cb)(Cb)^T + C\Gamma Q \Gamma^T C^T + R\}^{-1} \qquad (46)
\end{aligned}
$$

Finally,

$$P_{k+1_{(x,K)}} = P_{k_{(x,K)}} - KHP_{k_{(x,K)}} \qquad (47)$$

Hence, we calculate

$$
P_{k+1_{(x,K)}} = \begin{pmatrix} AP_{k_{xx}}A^T + u_k(Ap_{k_{xK}}b^T + \\ bp_{k_{xK}}^T A^T) + u_k^2 p_{k_{KK}} bb^T + \Gamma Q \Gamma^T & \vdots & Ap_{k_{xK}} + u_k p_{k_{KK}} b \\ \cdots\cdots\cdots\cdots\cdots\cdots\cdots\cdots & \vdots & \cdots\cdots\cdots\cdots \\ p_{k_{xK}}^T A^T + u_k p_{k_{KK}} b^T & \vdots & p_{k_{KK}} \end{pmatrix} -
$$

$$
\begin{pmatrix} \{AP_{k_{xx}}A^TC^T + u_k[Ap_{k_{xK}}(Cb)^T + b(CAp_{k_{xK}})^T] \\ +u_k^2 p_{k_{KK}} b(Cb)^T + \Gamma Q \Gamma^T C^T\} \times \{CAP_{k_{xx}}A^TC^T \\ +u_k[CAp_{k_{xK}}(Cb)^T + (Cb)(CAp_{k_{xK}})^T] + u_k^2 p_{k_{KK}}(Cb)(Cb)^T \\ +C\Gamma Q\Gamma^T C^T + R\}^{-1} \times [CAP_{k_{xx}}A^T + u_k(CAp_{k_{xK}}b^T \\ +Cbp_{k_{xK}}^T A^T) + u_k^2 p_{k_{KK}} Cbb^T + C\Gamma Q\Gamma^T] & \vdots \\ \cdots\cdots\cdots\cdots\cdots\cdots\cdots\cdots\cdots\cdots\cdots\cdots\cdots\cdots\cdots\cdots\cdots\cdots\cdots\cdots\cdots\cdots\cdots\cdots\cdots\cdots\cdots\cdots & \vdots \\ [(CAp_{k_{xK}})^T + u_k p_{k_{KK}}(Cb)^T] \times \{CAP_{k_{xx}}A^TC^T \\ +u_k[CAp_{k_{xK}}(Cb)^T + (Cb)(CAp_{k_{xK}})^T] + u_k^2 p_{k_{KK}}(Cb)(Cb)^T \\ +C\Gamma Q\Gamma^T C^T + R\}^{-1} \times [CAP_{k_{xx}}A^T + u_k(CAp_{k_{xK}}b^T \\ +Cbp_{k_{xK}}^T A^T) + u_k^2 p_{k_{KK}} Cbb^T + C\Gamma Q\Gamma^T] & \vdots \end{pmatrix}
$$

$$
\begin{pmatrix} \vdots & \\ & \{AP_{k_{xx}}A^TC^T + u_k[Ap_{k_{xK}}(Cb)^T + b(CAp_{k_{xK}})^T] \\ & +u_k^2 p_{k_{KK}} b(Cb)^T + \Gamma Q \Gamma^T C^T\} \times \{CAP_{k_{xx}}A^TC^T \\ & +u_k[CAp_{k_{xK}}(Cb)^T + (Cb)(CAp_{k_{xK}})^T] + u_k^2 p_{k_{KK}}(Cb)(Cb)^T \\ & +C\Gamma Q\Gamma^T C^T + R\}^{-1} \times (CAp_{k_{xK}} + u_k p_{k_{KK}}(Cb)) \\ \vdots & \\ \cdots\cdots\cdots\cdots\cdots\cdots\cdots\cdots\cdots\cdots\cdots\cdots\cdots\cdots\cdots\cdots\cdots\cdots\cdots\cdots\cdots\cdots\cdots\cdots\cdots\cdots\cdots\cdots & \\ & [(CAp_{k_{xK}})^T + u_k p_{k_{KK}}(Cb)^T] \times \{CAP_{k_{xx}}A^TC^T \\ & +u_k[CAp_{k_{xK}}(Cb)^T + (Cb)(CAp_{k_{xK}})^T] + u_k^2 p_{k_{KK}}(Cb)(Cb)^T \\ & +C\Gamma Q\Gamma^T C^T + R\}^{-1} \times (CAp_{k_{xK}} + u_k p_{k_{KK}}(Cb)) \\ \vdots & \end{pmatrix} \quad (48)
$$

Thus,

$$\begin{aligned} P_{k+1_{xx}} &= [AP_{k_{xx}}A^T + u_k(Ap_{k_{xK}}b^T + bp_{k_{xK}}^T A^T) + u_k^2 p_{k_{KK}} bb^T \\ &\quad +\Gamma Q\Gamma^T]\{[AP_{k_{xx}}A^T + u_k(Ap_{k_{xK}}b^T + bp_{k_{xK}}^T A^T) \\ &\quad + u_k^2 p_{k_{KK}} bb^T + \Gamma Q\Gamma^T]^{-1} - C^T\{CAP_{k_{xx}}A^T C^T \\ &\quad +u_k[CAp_{k_{xK}}(Cb)^T + (Cb)(CAp_{k_{xK}})^T] + u_k^2 p_{k_{KK}}(Cb)(Cb)^T \\ &\quad +C\Gamma Q\Gamma^T C^T + R\}^{-1}C\}[AP_{k_{xx}}A^T + u_k(Ap_{k_{xK}}b^T + bp_{k_{xK}}^T A^T) \\ &\quad +u_k^2 p_{k_{KK}} bb^T + \Gamma Q\Gamma^T] \end{aligned} \tag{49}$$

Next, recall the complete Matrix Inversion Lemma (MIL).

Lemma 2*Assume relevant matrices are compatible and invertible. Then*

$$(A_1 - A_2A_4^{-1}A_3)^{-1} = A_1^{-1} + A_1^{-1}A_2(A_4 - A_3A_1^{-1}A_2)^{-1}A_3A_1^{-1} \tag{50}$$

□

Applying the MIL to the expression in the outer curly brackets from Eq. (49), viz.,

$$\begin{aligned} &\{[AP_{k_{xx}}A^T + u_k(Ap_{k_{xK}}b^T + bp_{k_{xK}}^T A^T) + u_k^2 p_{k_{KK}} bb^T + \Gamma Q\Gamma^T]^{-1} \\ &-C^T\{CAP_{k_{xx}}A^T C^T + u_k[CAp_{k_{xK}}(Cb)^T + (Cb)(CAp_{k_{xK}})^T] \\ &+u_k^2 p_{k_{KK}}(Cb)(Cb)^T + C\Gamma Q\Gamma^T C^T + R\}^{-1}C\}^{-1} \end{aligned}$$

where we set

$$\begin{aligned} A_1 &= [AP_{k_{xx}}A^T + u_k(Ap_{k_{xK}}b^T + bp_{k_{xK}}^T A^T) + u_k^2 p_{k_{KK}} bb^T + \Gamma Q\Gamma^T]^{-1} \\ A_2 &= C^T \\ A_3 &= C \\ A_4 &= \{CAP_{k_{xx}}A^T C^T + u_k[CAp_{k_{xK}}(Cb)^T + (Cb)(CAp_{k_{xK}})^T] \\ &\quad +u_k^2 p_{k_{KK}}(Cb)(Cb)^T + C\Gamma Q\Gamma^T C^T + R\} \end{aligned}$$

we obtain

$$\{[AP_{k_{xx}}A^T + u_k(Ap_{k_{xK}}b^T + bp_{k_{xK}}^T A^T) + u_k^2 p_{k_{KK}} bb^T + \Gamma Q \Gamma^T]^{-1} - C^T\{CAP_{k_{xx}}A^T C^T$$

$$+u_k[CAp_{k_{xK}}(Cb)^T + (Cb)(CAp_{k_{xK}})^T] + u_k^2 p_{k_{KK}}(Cb)(Cb)^T + C\Gamma Q\Gamma^T C^T + R\}^{-1}C\}^{-1}$$

$$= [AP_{k_{xx}}A^T + u_k(Ap_{k_{xK}}b^T + bp_{k_{xK}}^T A^T) + u_k^2 p_{k_{KK}} bb^T + \Gamma Q\Gamma^T] + [AP_{k_{xx}}A^T$$

$$+u_k(Ap_{k_{xK}}b^T + bp_{k_{xK}}^T A^T) + u_k^2 p_{k_{KK}} bb^T + \Gamma Q\Gamma^T]C^T\{\{CAP_{k_{xx}}A^T C^T + u_k[CAp_{k_{xK}}(Cb)^T$$

$$+(Cb)(CAp_{k_{xK}})^T] + u_k^2 p_{k_{KK}}(Cb)(Cb)^T + C\Gamma Q\Gamma^T C^T + R\} - C[AP_{k_{xx}}A^T + u_k(Ap_{k_{xK}}b^T$$

$$+bp_{k_{xK}}^T A^T) + u_k^2 p_{k_{KK}} bb^T + \Gamma Q\Gamma^T]C^T\}^{-1}C[AP_{k_{xx}}A^T + u_k(Ap_{k_{xK}}b^T + bp_{k_{xK}}^T A^T)$$

$$+u_k^2 p_{k_{KK}} bb^T + \Gamma Q\Gamma^T]$$

Reducing the above gives

$$[AP_{k_{xx}}A^T + u_k(Ap_{k_{xK}}b^T + bp_{k_{xK}}^T A^T) + u_k^2 p_{k_{KK}} bb^T + \Gamma Q\Gamma^T]\{[AP_{k_{xx}}A^T + u_k(Ap_{k_{xK}}b^T$$

$$+bp_{k_{xK}}^T A^T) + u_k^2 p_{k_{KK}} bb^T + \Gamma Q\Gamma^T]^{-1} + C^T R^{-1}C\}[AP_{k_{xx}}A^T + u_k(Ap_{k_{xK}}b^T + bp_{k_{xK}}^T A^T)$$

$$+u_k^2 p_{k_{KK}} bb^T + \Gamma Q\Gamma^T]$$

Hence, Eq. (49) can now be reduced to:

$$\begin{aligned} P_{k+1_{xx}} &= \{[AP_{k_{xx}}A^T + u_k(Ap_{k_{xK}}b^T + bp_{k_{xK}}^T A^T) \\ &\quad + u_k^2 p_{k_{KK}} bb^T + \Gamma Q \Gamma^T]^{-1} + C^T R^{-1} C\}^{-1} \end{aligned} \tag{52}$$

In addition,

$$\begin{aligned} p_{k+1_{KK}} &= p_{k_{KK}} - [(CAp_{k_{xK}})^T + u_k p_{k_{KK}}(Cb)^T]\{CAP_{k_{xx}}A^T C^T \\ &\quad + u_k[CAp_{k_{xK}}(Cb)^T + (Cb)(CAp_{k_{xK}})^T] + u_k^2 p_{k_{KK}}(Cb)(Cb)^T \\ &\quad + C\Gamma Q \Gamma^T C^T + R\}^{-1}(CAp_{k_{xK}} + u_k p_{k_{KK}}(Cb)) \end{aligned} \tag{53}$$

and

$$\begin{aligned} p_{k+1_{xK}} &= Ap_{k_{xK}} + u_k p_{k_{KK}} b - \{AP_{k_{xx}}A^T C^T + u_k[Ap_{k_{xK}}(Cb)^T \\ &\quad + b(CAP_{k_{xK}})^T] + u_k^2 p_{k_{KK}} b(Cb)^T + \Gamma Q \Gamma^T C^T\} \times \\ &\quad \{CAP_{k_{xx}}A^T C^T + u_k[CAp_{k_{xK}}(Cb)^T + (Cb)(CAp_{k_{xK}})^T] \\ &\quad + u_k^2 p_{k_{KK}}(Cb)(Cb)^T + C\Gamma Q \Gamma^T C^T + R\}^{-1}(CAp_{k_{xK}} \\ &\quad + u_k p_{k_{KK}}(Cb)) \end{aligned} \tag{54}$$

We also partition the Kalman gain vector as follows

$$K = \begin{pmatrix} K_x \\ K_K \end{pmatrix} \tag{55}$$

where

$$\begin{aligned} K_x &= \{AP_{k_{xx}}A^T C^T + u_k[Ap_{k_{xK}}(Cb)^T + b(CAp_{k_{xK}})^T] \\ &\quad + u_k^2 p_{k_{KK}} b(Cb)^T + \Gamma Q \Gamma^T C^T\} \times CAP_{k_{xx}}A^T C^T \\ &\quad + u_k[CAp_{k_{xK}}(Cb)^T + (Cb)(CAp_{k_{xK}})^T] + u_k^2 p_{k_{KK}}(Cb)(Cb)^T \\ &\quad + C\Gamma Q \Gamma^T C^T + R\}^{-1} \end{aligned}$$

and

$$
\begin{aligned}
K_K &= [(CAp_{k_{xK}})^T + u_k p_{k_{KK}}(Cb)^T]\{CAP_{k_{xx}}A^TC^T \\
&\quad + u_k[CAp_{k_{xK}}(Cb)^T + (Cb)(CAp_{k_{xK}})^T] + u_k^2 p_{k_{KK}}(Cb)(Cb)^T \\
&\quad + C\Gamma Q\Gamma^T C^T + R\}^{-1} \qquad (57)
\end{aligned}
$$

Hence,

$$\hat{x}_{k+1} = A\hat{x}_k + \hat{K}_k b u_k + K_x(z_{k+1} - CA\hat{x}_k - \hat{K}_k Cbu_k) \qquad (58)$$

$$\hat{K}_{k+1} = \hat{K}_k + K_K(z_{k+1} - CA\hat{x}_k - \hat{K}_k Cbu_k) \qquad (59)$$

□

Remark 1 *An application of the MIL will reduce the number of matrix inversions such that only the low-order matrix*

$$CAP_{k_{xx}}A^TC^T + u_k[CAp_{k_{xK}}(Cb)^T + (Cb)(CAp_{k_{xK}})^T] + u_k^2 p_{k_{KK}}(Cb)(Cb)^T + C\Gamma Q\Gamma^T C^T + R$$

needs to be inverted.

4.3 Discussion

It is important to realize that the absence of complete plant information, viz., the uncertainty in the loop gain parameter K, causes both the loop gain and the state estimation error covariances to be dependent on the input signal - see, e.g., Eqs. (34)-(37). This is a major departure from the classical state estimation paradigm in linear control theory. Thus, the loop gain estimate $\hat{K}$ (and also the loop gain estimation error covariance) are now time dependent. Obviously, the best loop gain estimate is obtained at the end of the estimation interval, at time N. In addition, the algorithm-provided loop gain and state estimates are correlated. Furthermore, the loop gain and state estimates' dependence on the input signal is nonlinear. The input signal dependence of the loop gain and state estimation error covariances, is a unique manifestation of the dual control effect.

4.3.1 Special Example 1

Consider the classical Kalman Filter paradigm where K is known, i.e., K=1. In this special case

$$p_{o_{KK}} = 0, \qquad p_{o_{xK}} = 0, \qquad p_{k_{KK}} = 0, \qquad p_{k_{xK}} = 0 \qquad \text{for all } k = 1, 2, ...$$

and it follows that

$$P_k = P_{k_{xx}} \tag{60}$$

$$K_K = 0 \tag{61}$$

$$K_x = (AP_{k_{xx}}A^T + \Gamma Q \Gamma^T)C^T\{CAP_{k_{xx}}A^TC^T + C\Gamma Q\Gamma^T C^T + R\}^{-1} \tag{62}$$

$$P_{k+1_{xx}} = [(AP_{k_{xx}}A^T + \Gamma Q\Gamma^T)^{-1} + C^T R^{-1} C]^{-1} \tag{63}$$

Thus, the classical Kalman filter formulae are recovered.

□

Remark 2 *If x_o is known, viz., $x_o = N(\bar{x}_o, 0)$, i.e., $P_{o_x} = 0$, and only the loop gain parameter K is not known, i.e., $P_{o_{xx}} = 0$, $p_{o_{xK}} = 0$, one nevertheless has to deal with an uncertain x at time k (even if Γ=0 and if there is no process noise) and one must propagate* $\begin{pmatrix} \hat{x}_k \\ \hat{K}_k \end{pmatrix}$ *and* $P_{k_{(n+1)\times(n+1)}}$.

4.3.2 Special Example 2

Special case: C is a row vector (*i.e.*,a scalar measurement is being used).

Then the estimation algorithm is

$$\hat{x}_{k+1} = A\hat{x}_k + \hat{K}_k b u_k + K_x(z_{k+1} - CA\hat{x}_k - \hat{K}_k(Cb)u_k) \tag{64}$$

$$\hat{K}_{k+1} = \hat{K}_k + K_K(z_{k+1} - CA\hat{x}_k - \hat{K}_k(Cb)u_k) \tag{65}$$

where the Kalman gain for state estimation is:

$$K_x = \frac{1}{X}\{AP_{k_{xx}}A^TC^T + u_k[(Cb)Ap_{k_{xK}} + (CAp_{k_{xK}})b] + u_k^2(Cb)p_{k_{KK}}b + \Gamma Q\Gamma^TC^T\} \quad (66)$$

and where the scalar X is given by:

$$X \triangleq CAP_{k_{xx}}A^TC^T + 2u_k[(Cb)CAp_{k_{xK}} + u_k^2(Cb)^2p_{k_{KK}} + C\Gamma Q\Gamma^TC^T + R \quad (67)$$

The Kalman gain for loop gain estimation is

$$K_K = \frac{[CAp_{k_{xK}} + u_k(Cb)p_{k_{KK}}]}{X} \quad (68)$$

Finally, the estimation error covariances are

$$P_{k+1_{xx}} = \{[AP_{k_{xx}}A^T + u_k(Ap_{k_{xK}}b^T + bp_{k_{xK}}^TA^T) + u_k^2p_{k_{KK}}bb^T + \Gamma Q\Gamma^T]^{-1} + \frac{1}{R}C^TC\}^{-1} \quad (69)$$

$$p_{k+1_{KK}} = p_{k_{KK}} - \frac{[CAp_{k_{xK}} + u_k(Cb)p_{k_{KK}}]^2}{X} \quad (70)$$

$$p_{k+1_{xK}} = Ap_{k_{xK}} + u_kp_{k_{KK}}b - \frac{CAp_{k_{xK}} + u_k(Cb)p_{k_{KK}}}{X} \{AP_{k_{xx}}A^TC^T + u_k[(Cb)Ap_{k_{xK}} + (CAp_{k_{xK}})b] + u_k^2(Cb)p_{k_{KK}}b + \Gamma Q\Gamma^TC^T\} \quad (71)$$

4.4 Alternative, Batch Approach to Estimation

The system state

$$x_k = A^kx_o + K\sum_{i=0}^{k-1}A^{k-1-i}bu_i + \sum_{i=0}^{k-1}A^{k-1-i}\Gamma w_i, \qquad k = 1, 2, ...N-1 \quad (72)$$

and the measurement

$$Z_k = CA^k x_o + K\sum_{i=0}^{k-1} CA^{k-1-i}bu_i + \sum_{i=0}^{k-1} CA^{k-1-i}\Gamma w_i \tag{73a}$$

$$= \left[\begin{array}{cc} CA^k & \sum_{i=0}^{k-1} CA^{k-1-i}bu_i \end{array}\right]\left(\begin{array}{c} x_o \\ K \end{array}\right) + \left(\sum_{i=0}^{k-1} CA^{k-1-i}\Gamma w_i + \nu_i\right) \tag{73b}$$

This yields the linear regression

$$Z = H\Theta + \widetilde{V} \tag{74}$$

where

$$\Theta \triangleq \left(\begin{array}{c} x_o \\ K \end{array}\right)_{(n+1)\times 1} \tag{75a}$$

$$Z \triangleq \left(\begin{array}{c} Z_1 \\ \vdots \\ Z_{N-1} \end{array}\right)_{(N-1)\times 1} \tag{75b}$$

$$H \triangleq \left(\begin{array}{cc} CA & U_0Cb \\ \vdots & \vdots \\ CA^{N-1} & \sum_{i=0}^{N-2} u_{k-1-i}CA^ib \end{array}\right) \tag{75c}$$

$$\widetilde{V}_k \triangleq \sum_{i=0}^{k-1} CA^i\Gamma w_{k-1-i} + \nu_k \tag{75d}$$

$$\widetilde{R} \triangleq E(\widetilde{V}\widetilde{V}^T) \tag{75e}$$

where

$$\widetilde{R} = Diag\left(\begin{array}{c} \widetilde{r}_1 \\ \vdots \\ \widetilde{r}_{N-1} \end{array}\right) \tag{76}$$

and where

$$\widetilde{r}_k = \sum_{i=0}^{k-1} CA^iPQP^T(A^T)C^T + R. \tag{77}$$

The window length is N-1.

This linear regression is augmented by the prior information equations

$$\overline{x}_o = x_o + w_k, \qquad E(w_x w_x^T) = P_{ox} \tag{78a}$$

$$K_o = K + w_{k,} \qquad E(w_k^2) = P_{ok} \tag{78b}$$

i.e., the above linear regression is augmented to include

$$\begin{pmatrix} \overline{x}_o \\ K_o \end{pmatrix} = I_{N+1}\Theta + \widetilde{W} \tag{79a}$$

$$E(W\widetilde{W}^T) = \begin{pmatrix} P_{ox} & 0 \\ 0 & P_{oK} \end{pmatrix}_{(n+1)\times(n+1)} \tag{79b}$$

Hence, the augmented linear regression is

$$\begin{pmatrix} \overline{x}_0 \\ Z \end{pmatrix} = \begin{pmatrix} I_{N+1} \\ H \end{pmatrix}_{(N+n)\times(n+1)} \Theta + \begin{pmatrix} \widetilde{W} \\ \widetilde{V} \end{pmatrix} \tag{80}$$

where

$$E\left(\begin{pmatrix} \widetilde{W} \\ \widetilde{V} \end{pmatrix}\begin{pmatrix} \widetilde{W}^T & \widetilde{V}^T \end{pmatrix}\right) = \begin{pmatrix} P_{0x} & 0 & 0 \\ 0 & P_{0k} & 0 \\ 0 & 0 & Diag(\widetilde{r}_k) \end{pmatrix}_{(N+n)\times(N+n)} \tag{81}$$

In summary, a system identification algorithm was developed to identify a systems' loop gain, K. A proof of this theorem, was given and supporting examples discussed. An alternative batch approach to loop gain estimation was also given.

Chapter 5 - Results

5.1 Zero Order Hold

The commanded pitch rate is a continuous signal created by the pilots' force on the stick. The signal is fed into the plant and is passed through a analog to digital (A/D) converter and is sampled. This digital response contains a delay caused by the hold in the sample process. A delay in the feedback loop corrupts the damping and stability of the system. This delay is shown to be represented [9] using a first order approximation where the continuous signal lags the sampled signal by $\frac{T}{2}$

$$G(S) = \frac{2/T}{s + 2/T}$$

where T is the sample period and 1/T is the sample rate given as cycles per second or Hz. When the signal, u(t), is being sampled at every kT points, $0 \leq k \leq \infty$, the value of the signal at u(kT) is held to the next sample point (k+1)T. This gives a "stair case" estimate of the signal. Using the first harmonic approximation, which is essentially the average of the sampled signal u(kT), we get the input signal. However, the new signal is shifted, or delayed, by the size of the sample period. The following figure shows how the digital control system delays a signal following a step input. When the sample period is decreased, the delay gets smaller and follows the continuous signal more exactly - see, e.g., Figs. 11 and 12.

5.2 Experimental Setup and Tracking Control

One would like a feedback control system to be robust enough to perform within specifications in the face of parametric uncertainty, e.g., control surface loss due to failures. As the critical open-loop gain K decreases from one to zero, which represents a transition from no failure to complete control surface loss, the tracking of the reference signal begins to slip. Even though failure, viz., a reduction in the control derivative, causes a fixed controller's tracking performance to deteriorate,

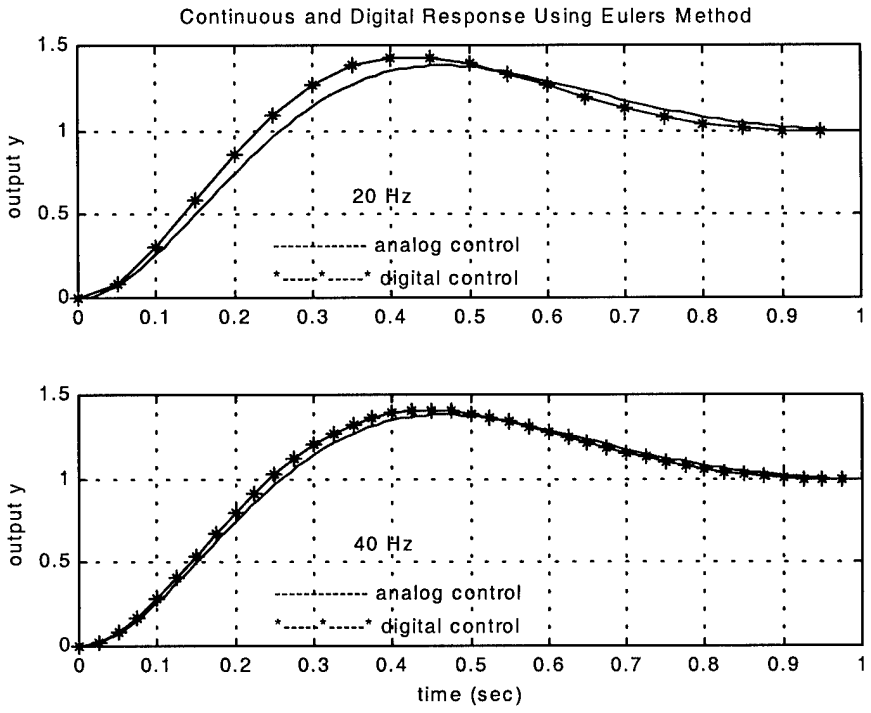

Figure 11. Continuous and digital response for a step input [9].

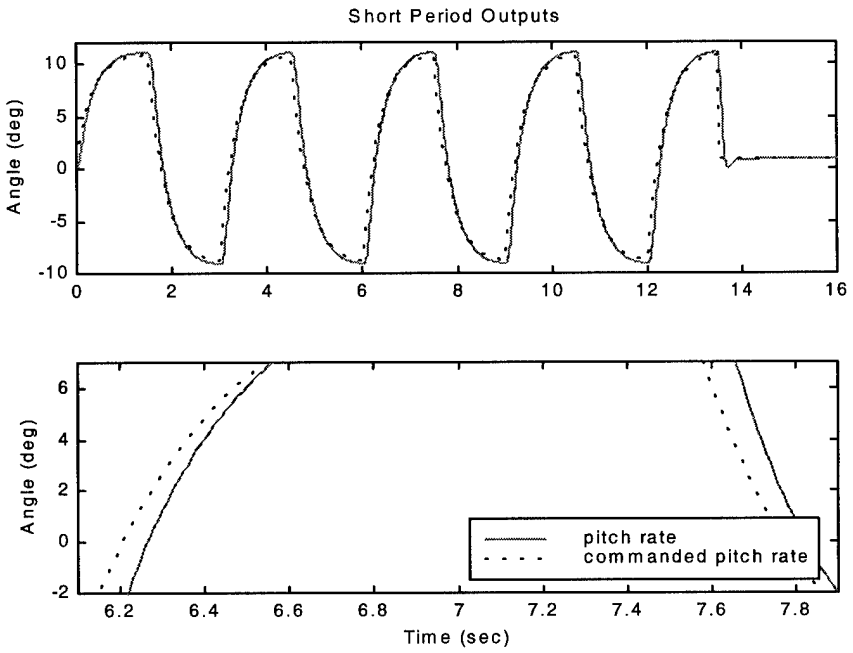

Figure 12. Efects of discritization on the commanded continuous input; Pitch rate is the discrete signal

still, a correct system identification algorithm will properly estimate the degree of failure. Hence, one is motivated to use on-line system identification and adjust the controller's gain on line in order to account for the failure-induced reduction in open-loop gain, thus achieving adaptive and reconfigurable control.

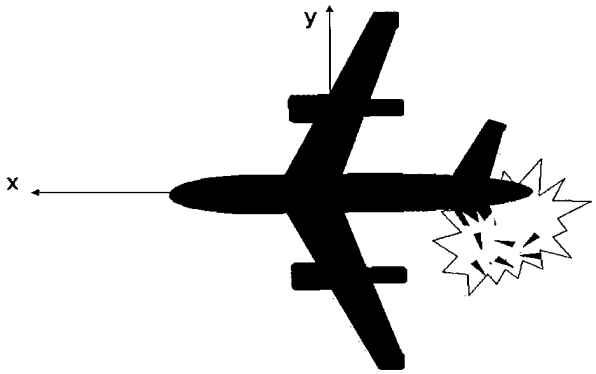

Figure 13. Aircraft elevator damage

In our simulation, a control surface failure is induced at 4.5 seconds into the flight for all the test runs. This translates into a jump in K from 1 to K=K_1, 0<K_1<1. Hence, the degree of failure is parameterized by K_1.

In addition, measurement (sensor) noise is injected into the simulation. Thus, the measured pitch rate is $q_m = q + v_q$, where $v_q = N(0, \sigma_q^2)$, and the measured angle of attack is $\alpha_m = \alpha + v_\alpha$, where $v_\alpha = N(0, \sigma_\alpha^2)$. Given that both α and q observations are used for system identification, the following definition of SNR is used:

$$SNR \triangleq 20 \log \sqrt{\left(\frac{\alpha_{\max}^2 + w^2 q_{\max}^2}{2\left(\sigma_\alpha^2 + w^2 \sigma_q^2\right)} \right)} \tag{82}$$

where the weighting

$$w = \frac{1}{\sqrt{|p_1 p_2|}} [\text{sec}]$$

and p_1, p_2 are the poles of the open-loop plant (the short period approximation):

$$p_1 = -0.6737 \qquad p_2 = 0.30691$$

In our simulations,

$$\alpha_{\max} \approx 6^\circ, \qquad q_{\max} \approx 11^\circ.$$

The experimental results presented in Figs. 14–31 were obtained using a fixed σ_α=0.03 deg.

For the SNR experiments of 40 and 60 dB, a scaled σ_q and σ_α are used. We initially let $\sigma_q = 0.05\,\text{deg}/\,\text{sec}$, and $\sigma_\alpha = 0.05\,\text{deg}$ and we set

$$\sigma_q = k\sigma_q \tag{83a}$$

$$\sigma_\alpha = k\sigma_\alpha \tag{83b}$$

where the SNR scaling parameter k > 0. The SNR is now expressed as

$$SNR(k) \triangleq 20\log\sqrt{\left(\frac{\alpha_{\max}^2 + \mathrm{w}^2 q_{\max}^2}{2\left(\sigma_\alpha^2 + \mathrm{w}^2\sigma_q^2\right)k^2}\right)} \tag{84}$$

and therefore, for a specified SNR, the parameter k is determined according to

$$k = \sqrt{\frac{\alpha_{\max}^2 + \mathrm{w}^2 q_{\max}^2}{2\left(\sigma_\alpha^2 + \mathrm{w}^2\sigma_q^2\right)}} \bullet 10^{-\frac{SNR}{20}}$$

and in the simulation experiments σ_q and σ_α are adjusted according to Eqs. (83a) and (83b), respectively. The σ_q, σ_α and SNR values are shown in Table 1.

Table 1. SNR values using a constant σ_α=0.03 deg

σ_q deg/sec	σ_α deg	SNR dB
0.55534	0.03	23.29
0.1108	0.03	37.227
0.0739	0.739	40
0.01108	0.03	53.286
0.00739	0.00739	60

5.2.1 Tracking Control

The F-16 class plant is open-loop unstable. This is a normal characteristic of advanced fighter aircraft. Using full state feedback, the flight control system can be stabilized. The ensuing closed loop linear state feedback control system is very robust; a well designed robust tracking controller can handle an open-loop gain as low as K=0.08. At lower K values, the feedback stabilization action becomes ineffective and the closed loop system becomes unstable. In this work, two tracking controllers are considered, a Proportional and Integral (PI) controller and a proportional controller.

5.2.1.1 PI Controller

Tracking is achieved using a fixed PI controller. The control law is

$$\delta_{e_c} = r - K_\alpha \alpha - K_q q - K_{\delta_e} \delta_e + K_z z$$

where the reference signal is the commanded pitch rate $r=q_c$, and where z is the "charge" on the integrator of the PI controller. The controller gains are K_z = -0.0001, K_α = 0.283, K_q= 0.876 and K_{δ_e} = -0.4. Table 1 shows the eigenvalues of the open-loop plant and the closed-loop system when this PI controller is used for tracking control.

Table 2. Longitudinal dynamics

Open-loop Plant	Closed-loop System, K=1	Closed-loop System, K=0.08
N/A	-14.4614+15.504j	-26.6776
0.6737	-14.4614-15.504j	-3.7210
-3.0691	-1.4724	0.0016 + 0.0071j
-20.0	0	0.0016 - 0.0071j

As can be seen, the bare plant is originally open-loop unstable. State feedback stabilizes the α, q, and δ_e states of the unimpaired closed-loop flight control system. As the critical loop gain K is lowered from a value of 1, which corresponds to having no failure, to an almost complete longitudinal control surface loss at a value of K≈0.08, the closed-loop system reverts to instability again.

In the tracking control experiments the above designed fixed PI controller is used. In the simulations, at time t=4.5 sec. into the flight, the open-loop gain K is reduced to $K = K_1$ =0.8, $K = K_1$ =0.6, $K = K_1$ =0.4, $K = K_1$ =0.2 and $K = K_1$ =0.1. Although no loss in post-failure tracking performance is recorded for K_1=0.8 in Fig. 14 (due to the robustness of the controller), a discernible loss in tracking performance is evident for K_1=0.6, as is shown in Fig. 15, and the degradation in tracking performance is more pronounced for K_1=0.4 and K_1=0.2 in Figs. 16 and 17, respectively. Although the control system does not become unstable until a degree of failure which corresponds to K_1=0.08, the post-failure tracking performance of the PI controller falls out of acceptable limits before this point, approximately when the loop gain $K_1 \leq 0.25$ - see, e.g. Fig. 17, where the results for K_1=0.2 are shown. When the K value decreases further to K_1=0.1 and below, as shown in Fig. 18, post-failure tracking performance of the fixed controller deteriorates greatly, although stability is still preserved until K_1=0.08.

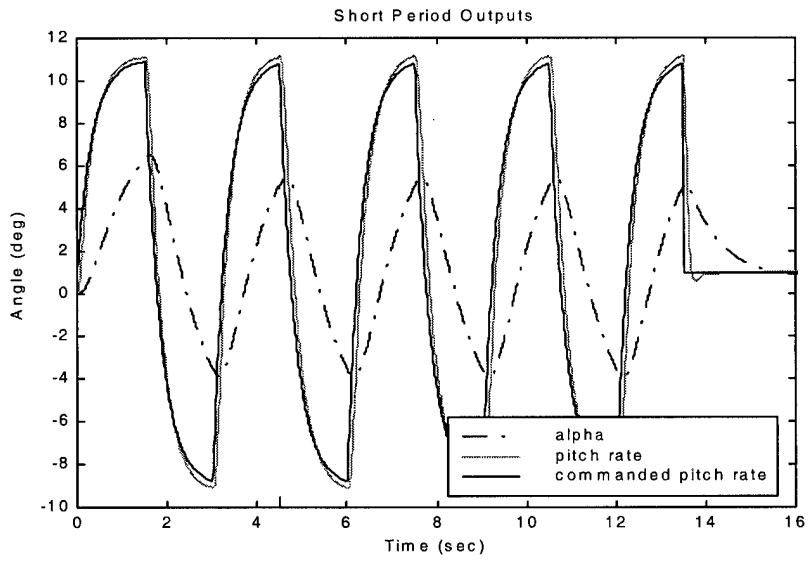

Figure 14. Pitch rate and alpha response for a loop gain of K_1=0.8, $\sigma_q = 0.1108\,\text{deg/sec}$, $\sigma_\alpha = 0.03\,\text{deg}$ and SNR=37.227 dB

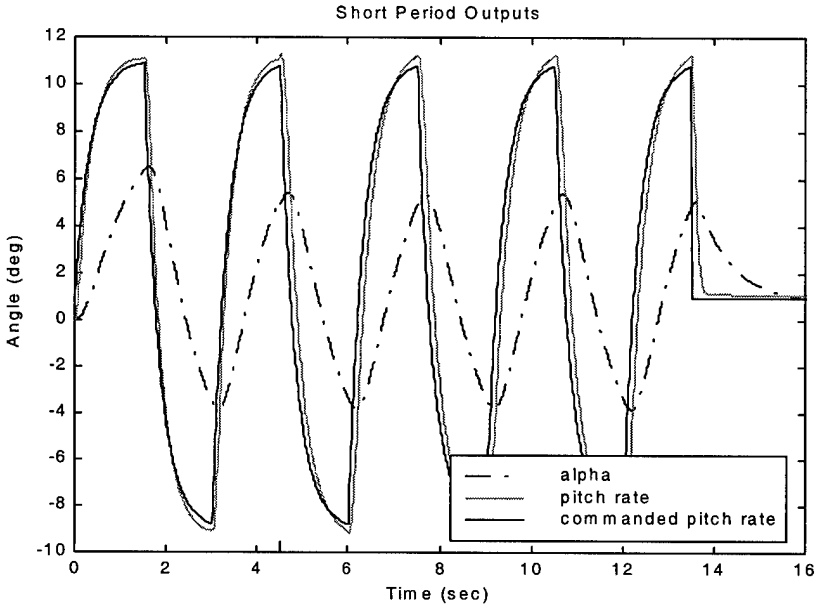

Figure 15. Pitch rate and alpha response for a loop gain of K_1=0.6, $\sigma_q = 0.1108\,\text{deg/sec}$, $\sigma_\alpha = 0.03\,\text{deg}$ and SNR=37.227 dB

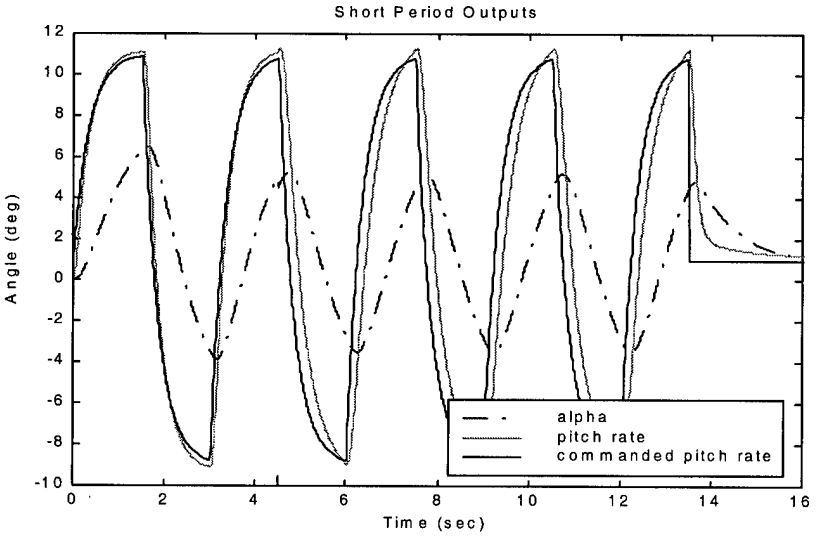

Figure 16. Pitch rate and alpha response for a loop gain of K_1=0.4, $\sigma_q = 0.1108\,\text{deg/sec}$, $\sigma_\alpha = 0.03\,\text{deg}$ and SNR=37.227 dB

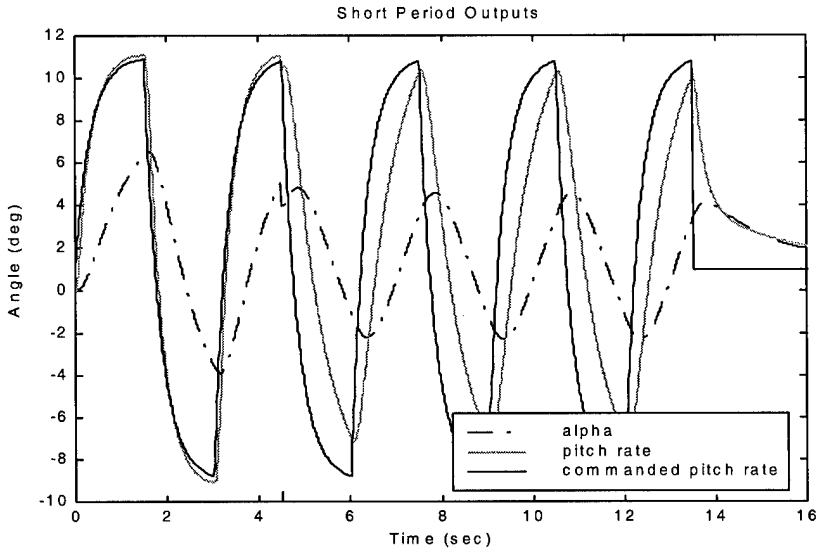

Figure 17. Pitch rate and alpha response for a loop gain of K_1=0.2, $\sigma_q = 0.1108\,\text{deg/sec}$, $\sigma_\alpha = 0.03\,\text{deg}$ and SNR=37.227 dB

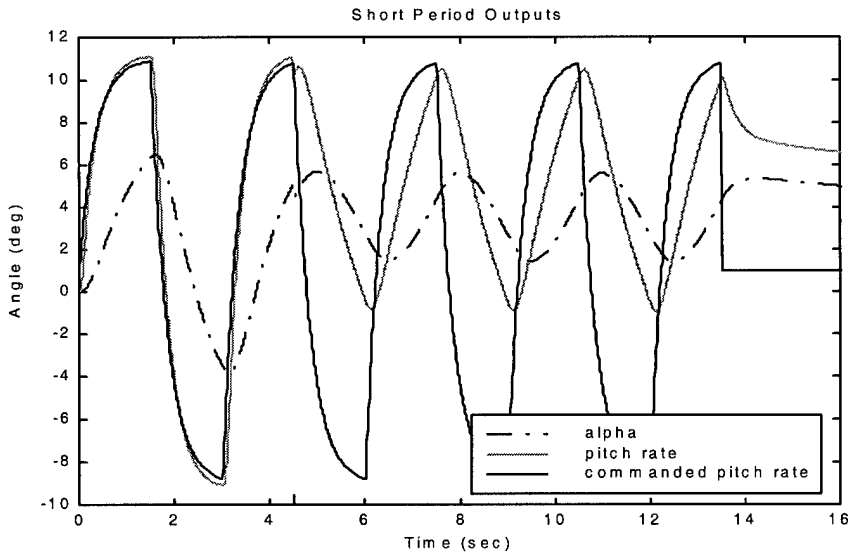

Figure 18. Pitch rate and alpha response for a loop gain of K_1=0.1, $\sigma_q = 0.1108\,\text{deg/sec}$, $\sigma_\alpha = 0.03\,\text{deg}$ and SNR=37.227 dB

Figs. 19 and 20 show the state estimates, as calculated from the system identification algorithm, for a degree of failure of K_1=0.8 and K_1=0.2. After the point of failure, some error between the estimated pitch rate and the commanded pitch rate can be seen. The state estimates improve as time increases, converging back to the true commanded pitch rate. When the degree of failure increases to K_1=0.2, the pitch rate estimate error also increases. With the low SNR and high degree of failure, the system identification algorithm shows some degradation of estimation performance. The loop gain K estimation performance wil be shown in the next Section.

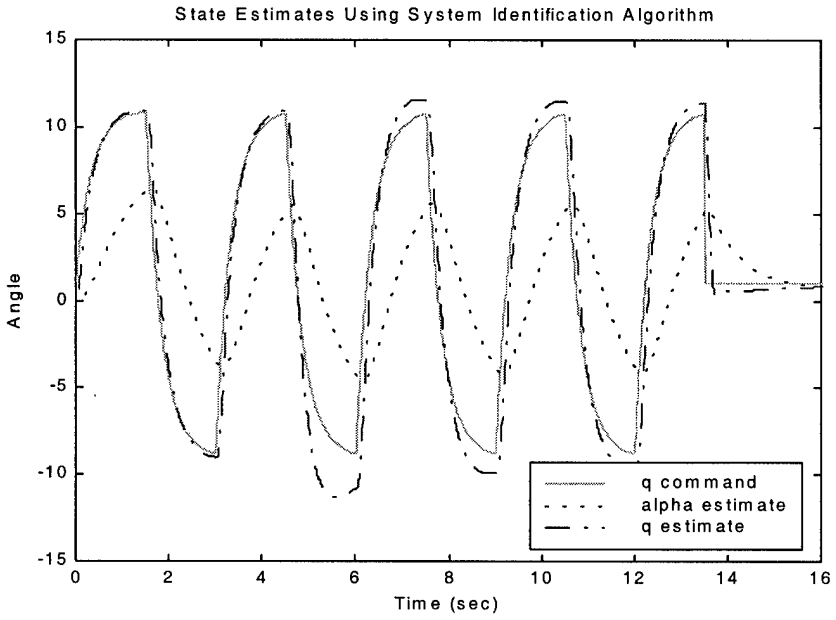

Figure 19. Pitch rate and alpha estimates; K_1=0.8, $\sigma_q = 0.1108\,\mathrm{deg/sec}$, $\sigma_\alpha = 0.03\,\mathrm{deg}$ and SNR=37.227 dB

5.2.1.2 Proportional Controller

Tracking is achieved using a fixed proportional controller. The control law is $\delta_{e_c} = K_r r - K_\alpha \alpha - K_q q - K_{\delta_e}$ where the reference signal r=q_c. The controller's gains are K_r= 0.9964, K_α = 0.283, K_q = 0.876 and $K_{\delta e}$ = -0.4. Integral action is not used to enforce tracking. The following table shows the eigenvalues of the closed-loop system using the proportional tracking controller.

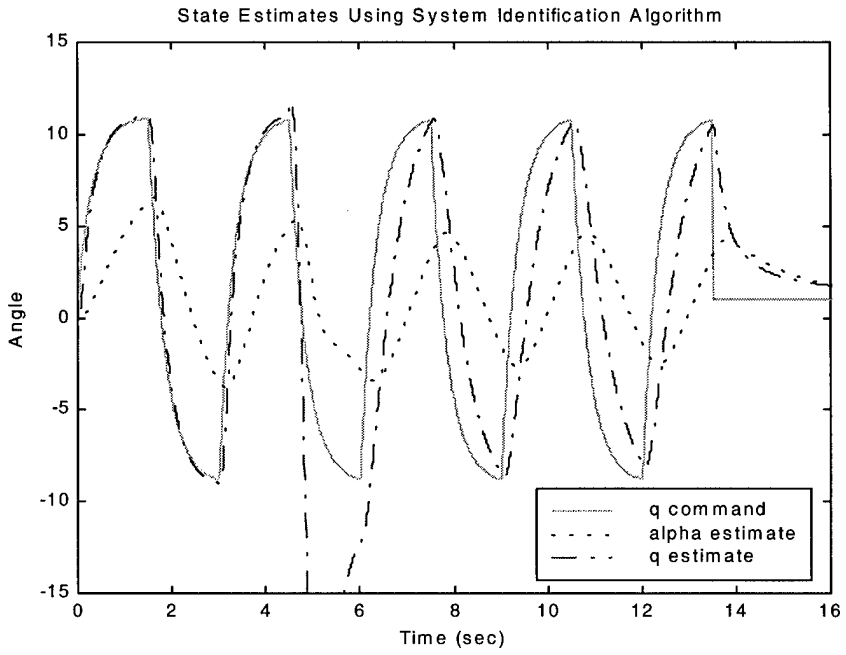

Figure 20. Pitch rate and alpha estimates; K_1=0.2, $\sigma_q = 0.1108\,\text{deg}/\text{sec}$, $\sigma_\alpha = 0.03\,\text{deg}$ and SNR=37.227 dB

Table 3. Longitudinal Dynamics

Open-loop (Short Period) Plant	Closed-loop System, K=1	Closed-loop System, K=0.08
-3.0691	-1.4724	0.0032
0.6737	-14.4615 +15.5040j	-3.7210
-20.0	-14.4615 -15.5040j	-26.6776

Once again, the open-loop plant is unstable and feedback stabilization is used. The closed-loop system becomes unstable again when the degree of control surface loss becomes excessively large, viz., K_1=0.08.

In general, post failure tracking performance of the fixed proportional controller for the various reduced open-loop gain values is similar to that of the PI controller. The post failure tracking performance of the proportional controller becomes unacceptable when the critical loop gain is reduced to K_1=0.2. When the critical loop gain is further reduced, tracking performance deteriorates rapidly as shown in Figs. 21 and 22. In both cases, when either the PI tracking controller or the proportional tracking controller were used, very similar identification results were obtained. Hence, the identification results for the PI controller only are displayed

5.3 Estimation Performance

When a fixed linear proportional or PI tracking controller is used and a severe failure occurs, the output signal of the plant (q) fails to follow the pitch rate command signal from the pilot (the reference signal q_c). However, even in the case of severe control surface loss the system identification algorithm (Theorem 1) still correctly estimates the value of the critical open-loop gain parameter K.

In this section, the estimation performance guaranteed by the novel system identification algorithm stated in Theorem 1 is experimentally investigated, and the results of the open-loop gain identification experiments are presented. The plant truth model used in the system identification

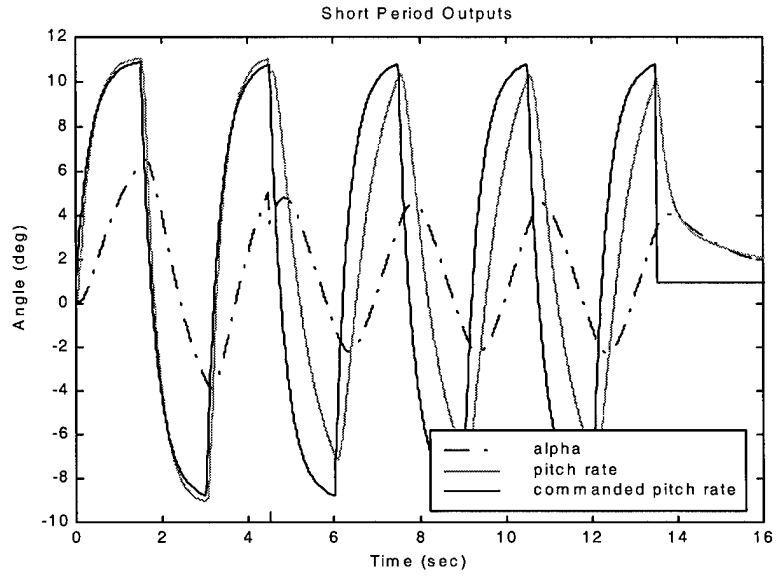

Figure 21. Pitch rate and alpha response for a loop gain of K_1=0.2, $\sigma_q = 0.1108\,\text{deg/sec}$, $\sigma_\alpha = 0.03\,\text{deg}$ and SNR=37.227 dB

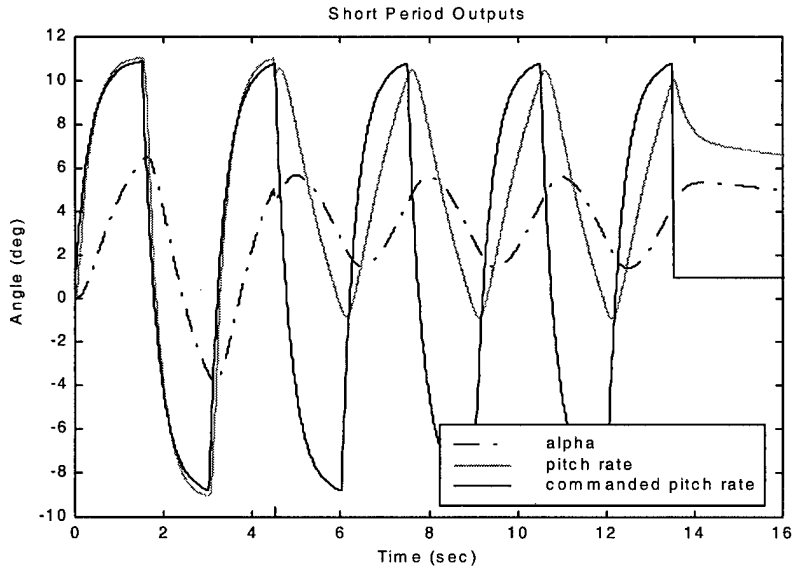

Figure 22. Pitch rate and alpha response for a loop gain of K_1=0.1, $\sigma_q = 0.1108\,\text{deg/sec}$, $\sigma_\alpha = 0.03\,\text{deg}$ and SNR=37.227 dB

algorithm is

$$\dot{\alpha} = Z_\alpha \alpha + Z_q q + K Z_{\delta_e} u$$

$$\dot{q} = M_\alpha \alpha + M_q q + K M_{\delta_e} u$$

viz., the state $\begin{pmatrix} \alpha \\ q \end{pmatrix}$ evolves in $\Re^2$ and the control signal is u=δ_e. A discrete-time version of the plant which corresponds to a sampling rate of 100Hz is embedded in the system identification algorithm. Furthermore, the prior parameter information given to the system identification algorithm is intentionally selected to be poor. It therefore takes the system identification algorithm some time to settle down and output the correct parameter estimates.

The system identification algorithm is able to estimate the open-loop gain for a high degree of failure, even in the presence of poor tracking. This is due to the system's enhanced excitation which is caused by poor tracking and is therefore conducive to good system identification. Figs. 23-27 show how the system identification algorithm using the expanding horizon Kalman filter (Theorem 1) estimates the open-loop gain K as the degree of failure increases. Because of the robustness of the linear controllers, both yielded similar tracking performance and thus similar identification performance. The results for both types of controllers are summarized in Table 4. The true and the identified open-loop gain K (for both the PI and the proportional tracking controller mechanizations) are shown.

Table 4. Open-Loop Gain Estimation Performance Analysis for Failure time of 4.5 sec

Actual Post Failure Open-Loop Gain	Final Estimated Value $\hat{K}$	Relative Estimation Error (%)	Settling Time (sec) for 20% Gain Estimation Error
0.8	0.8413	4.91	t_s=0.82
0.6	0.6469	7.25	t_s=1.93
0.4	0.4306	7.11	t_s=2.71
0.2	0.2116	5.48	t_s=1.83
0.1	0.0996	0.40	t_s=1.51

The identification settling time, t_s, when the expanding horizon estimate algorithm is used, is dependent on the degree of failure. Thus, a fairly good (20% error) estimate of the open-loop gain is obtained within 2.71 seconds after the failure. These estimates were obtained using an expanding data window with a relatively low SNR=37.227 dB. It will be shown in the next section how the identification time can be reduced using a moving window system identification algorithm.

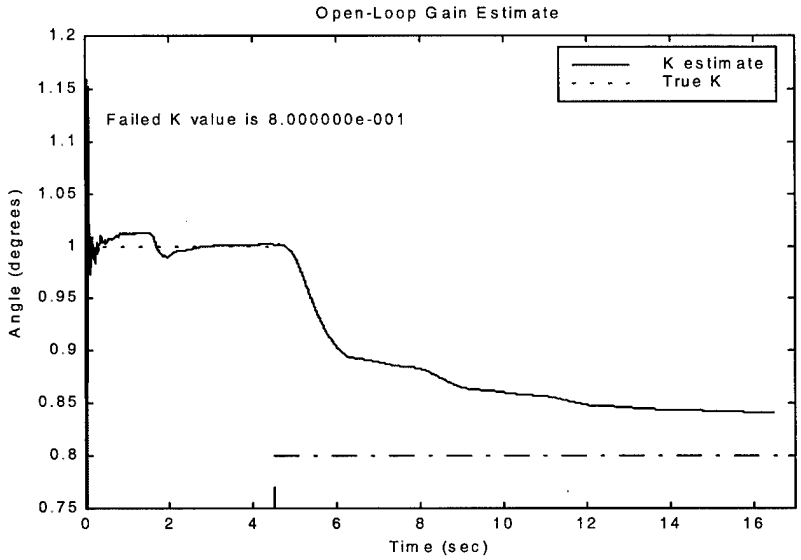

Figure 23. Open-loop gain estimimation for a failure of K_1=0.8, $\sigma_q = 0.1108\,\text{deg}/\text{sec}$, $\sigma_\alpha = 0.03\,\text{deg}$ and SNR=37.227 dB

5.4 Moving Window Estimation

A moving window (or, equivalently, finite memory data window) is used because in the case of a failure, when a jump in the value of the open-loop gain K occurs, the latter is identified faster than in the case where the expanding horizon system identification algorithm is used. By using the recursive system identification algorithm (Theorem 1) inside a 0.3 second window (of 30 samples), estimates of the parameters of interest are calculated. The window is then shifted one sample time and the estimation is repeated. This gives the first parameter estimate at 0.3 seconds into the

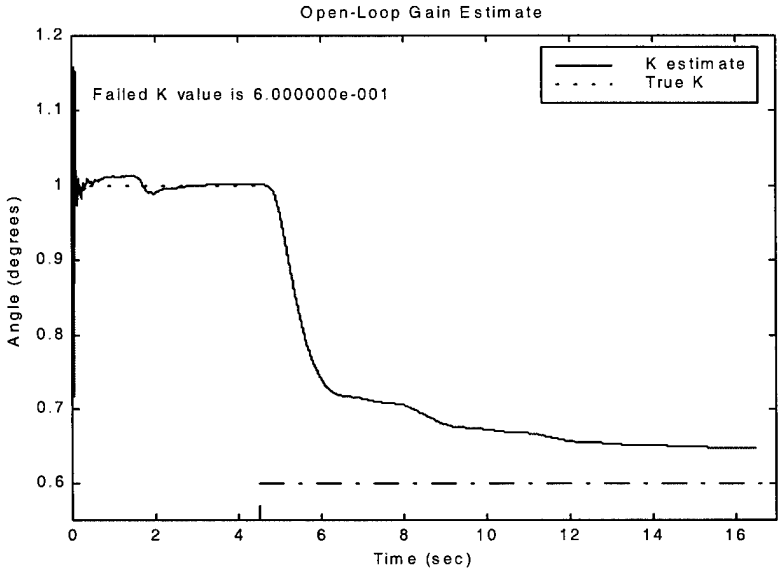

Figure 24. Open-loop gain estimimation for a failure of K_1=0.6, $\sigma_q = 0.1108\,\text{deg}/\text{sec}$, $\sigma_\alpha = 0.03\,\text{deg}$ and SNR=37.227 dB

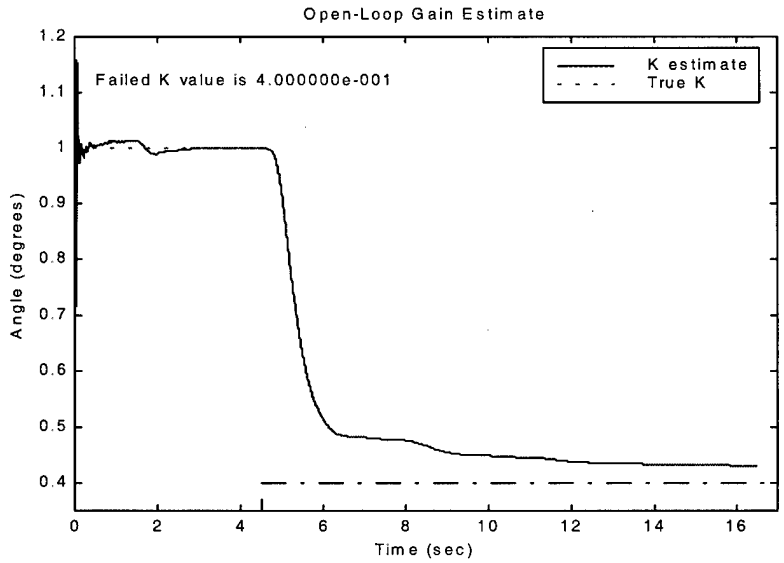

Figure 25. Open-loop gain estimimation for a failure of K_1=0.4, $\sigma_q = 0.1108\,\text{deg}/\text{sec}$, $\sigma_\alpha = 0.03\,\text{deg}$ and SNR=37.227 dB

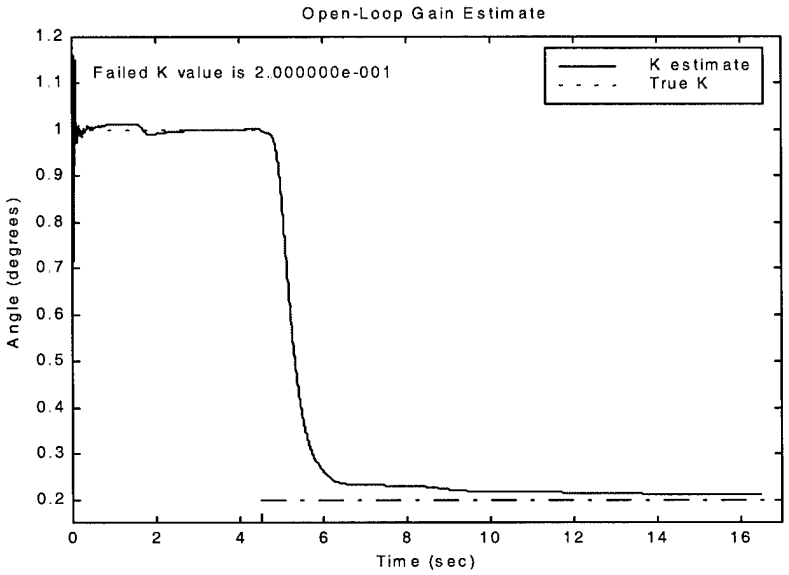

Figure 26. Open-loop gain estimimation for a failure of K_1=0.2, $\sigma_q = 0.1108\,\text{deg}/\text{sec}$, $\sigma_\alpha = 0.03\,\text{deg}$ and SNR=37.227 dB

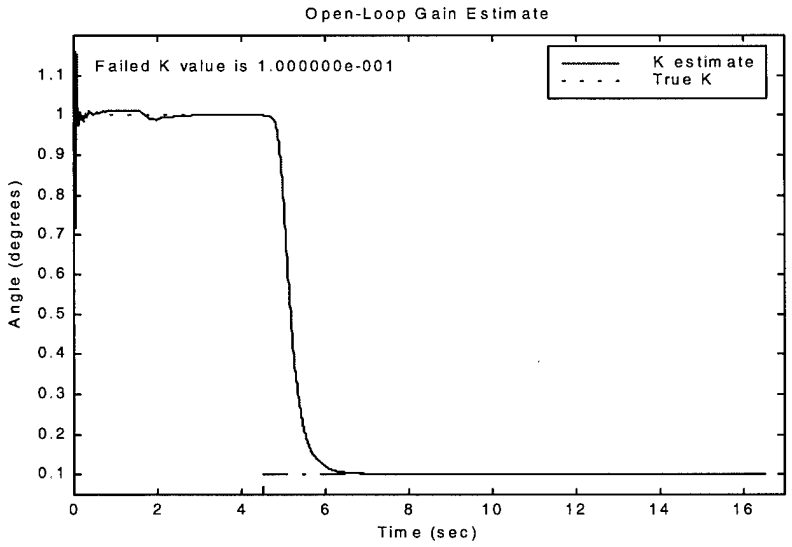

Figure 27. Open-loop gain estimimation for a failure of K_1=0.1, $\sigma_q = 0.1108\,\text{deg}/\text{sec}$, $\sigma_\alpha = 0.03\,\text{deg}$ and SNR=37.227 dB

flight. For all of the windows, the same prior information of $\alpha = -1.4414$ degrees, $q = -2.4314$ degrees/second, and the open-loop gain $K_1 = 0.8$, are used. Prior information with negative α and q was intentionally used to test the windowed estimation algorithm's response to a poor initial guess. The initial variances are 0.1 [deg^2], 1$\left[(\text{deg/sec})^2\right]$, and 0.4, respectively.

In Fig. 28, the dashed lines represent $\pm 20\%$ error from the true degree of failure. One can see that the moving window is quicker to settle on an estimate, while the expanding horizon system identification algorithm takes more time to reach its final estimate value. Obviously, the estimate provided by the expanding Kalman filter is smoother than the estimate provided by our relatively short sliding window. At the same time, the deleterious effect on estimation performance of a very short window ($\ll 0.3$ sec) is also evident near t=0 in the expanding horizon plots in Figs. 23-27.

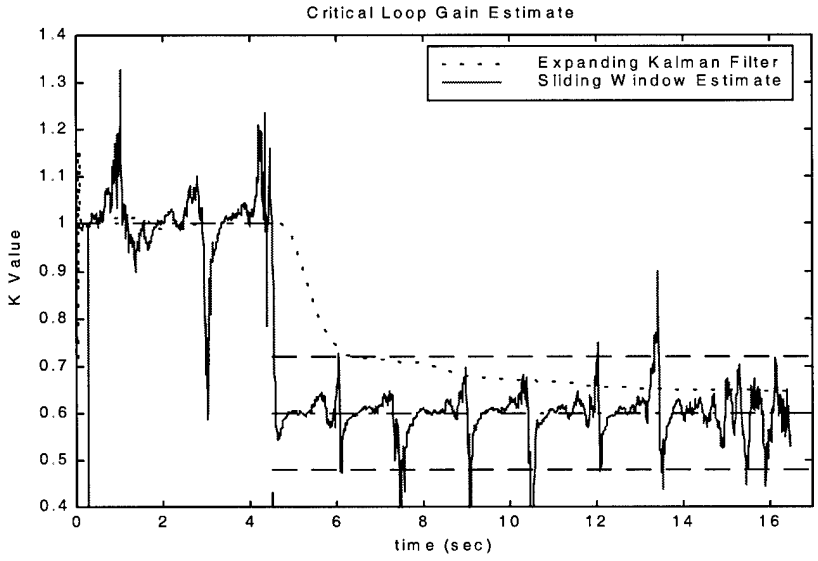

Figure 28. Expanding horizon versus moving window estimation; K_1=0.6, $\sigma_q = 0.1108\,\text{deg}/\text{sec}$, $\sigma_\alpha = 0.03\,\text{deg}$ and SNR=37.227 dB

Also note that when the moving window system identification algorithm is used, during certain windows, the excitation in the window is poor and these particular windows yield bad parameter estimates. These "poor" estimates occur when the window slides past the peaks of the input

command, as shown in Fig. 29. The peaks in the estimate seem to be correlated to the input peaks, as is evident in Fig. 29. Indeed, the input signal strongly affects the estimation performance of the system identification algorithm - as opposed to classical linear state estimation, i.e., Kalman filtering. Obviously, poor estimates are also recorded during periods of low control activity as is the case for 14<t<16 sec..

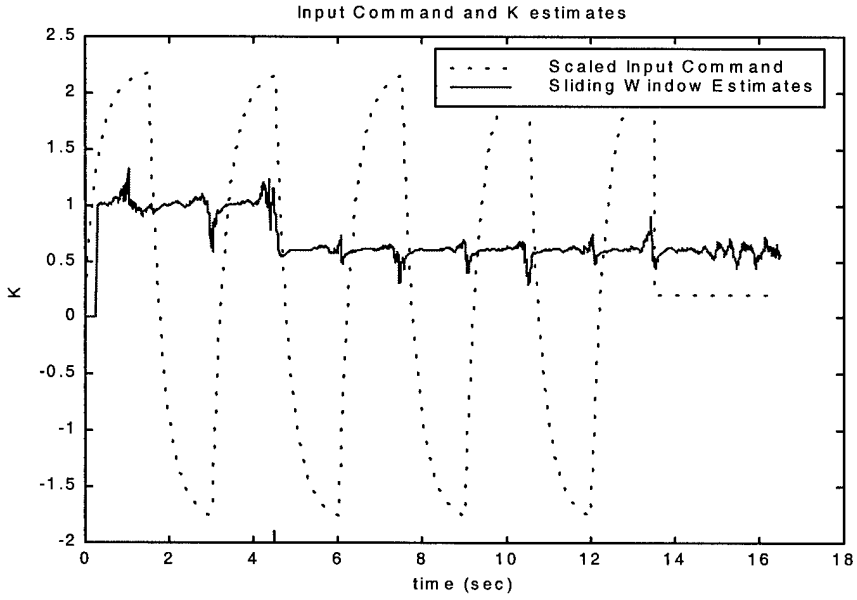

Figure 29. Input command versus the sliding window $\hat{K}$ estimate; K_1=0.6, $\sigma_q = 0.1108\,\text{deg}/\text{sec}$, $\sigma_\alpha = 0.03\,\text{deg}$ and SNR=37.227 dB

To reduce the fluctuations in the $\hat{K}$ estimates, the estimates output by the identification algorithm are smoothed through a first order low pass filter:

$$\hat{K}_{k_{smoothed}} = .9 * \hat{K}_{k-1_{smoothed}} + .1 * \hat{K}_k \tag{85}$$

Thus, the current estimate is given less weight than the previous estimate. Smoothing of the algorithm's output (estimates) helps to reduce the deleterious effects of noise and improve estimation performance. However, smoothing increases the identification time, which is of particular importance in a failure scenario. In Fig 30, the loop gain estimates are smoothed using various gains. As

can be seen, when $\hat{K}_{k_{smoothed}} = .7 * \hat{K}_{k-1_{smoothed}} + .3 * \hat{K}_k$ is used, the delay in detection time is greater than the unsmoothed estimates but less than when the smoothing gains in Eq. (85) is used. A reduction in detection delay comes at the expense of less smoothing. One must decide if this

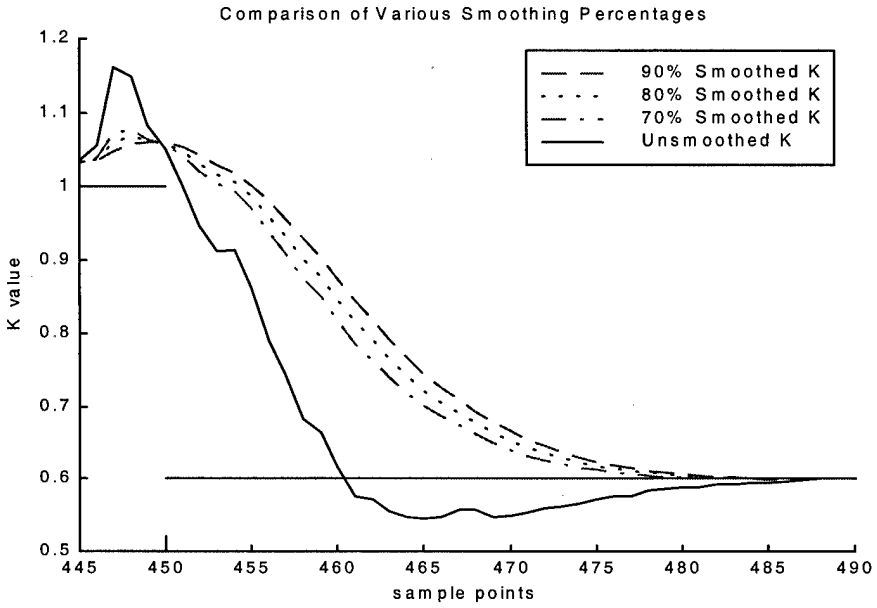

Figure 30. The effects of smoothing on failure detection time; K_1=0.6 and SNR=37.227 dB

is an appropriate trade-off. If smoothing is not an option then increasing the window length also helps to reduce the deleterious effect's of noise, and hence the fluctuations in the open-loop gain estimate $\hat{K}$ are reduced, but not as effectively. In this work, the loop gain estimates are smoothed using Eq. (85). Fig. 31 shows the effects of smoothing on the loop gain estimate. The dashed lines, once again, represent a $\pm 20\%$ error of the true loop gain, K.

Table 5 shows the time needed to obtain an open-loop gain estimate that is within 20% of the true open-loop gain using the windowed system identification algorithm. The open-loop gain estimates are calculated using a moving window and are smoothed. It is shown that, as the failure degree increases (K gets smaller), the time needed to identify the open-loop gain within $\pm 20\%$ of the true value, increases. As expected, the smoothed open-loop gain estimates require more time

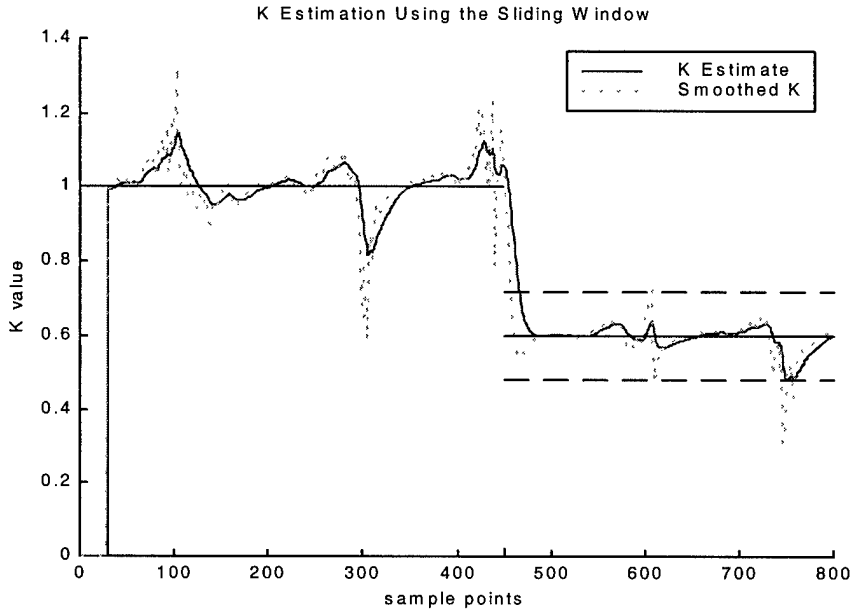

Figure 31. Open-loop gain estimates and smoothed open-loop gain estimates; K_1=0.6, $\sigma_q = 0.1108\,\text{deg}/\text{sec}$, $\sigma_\alpha = 0.03\,\text{deg}$ and SNR=37.227 dB

for identification than the original moving window algorithm provided estimates. An estimate of the open-loop gain with an error of less than 20% can be obtained after 0.23 seconds using the moving window, and it takes 0.5 seconds when the estimates are low pass filtered using Eq. (85). Nevertheless, this corresponds to a shortened identification time, viz., a reduction of over 1 second in identification time is obtained when compared to the expanding horizon algorithm's results in Table 4. Now, the settling time t_s is monotonic in the degree of failure, as expected.

Table 5. Time to Reach 20 Percent of True Loop Gain After Failure at 4.5 sec

Actual Open-Loop Gain After Failure	Settling Time for 20% Gain Estimation Error Using Moving Window	Settling Time for 20% Gain Estimation Error Using Moving Window with Smoothing
0.8	t_s=0.02	t_s=0.09
0.6	t_s=0.08	t_s=0.17
0.4	t_s=0.12	t_s=0.26
0.2	t_s=0.19	t_s=0.44
0.1	t_s=0.23	t_s=0.51

5.5 SNR Effects

The measurement noise intensity has a strong influence on how the moving window system identification algorithm estimates the plant's open-loop gain. In the previous figures, a SNR of 37.227 dB was universally used. When the SNR is increased to 53.286 dB, the identification performance improves and the estimates are smoother - see Fig. 32. However, when the SNR is lowered to 23.29 dB, the identification performance deteriorates and estimates become more erratic and peaks become more prominent, especially for windows that contain the instant of failure at t = 4.5 sec. - see, for example, Fig. 33. Thus, the SNR has a strong influence on the system identification algorithm's ability to estimate the parameters.

In Fig. 34, $K \pm 2\sigma$, where the predicted open-loop gain estimation error standard deviation $\sigma = \sqrt{p_{k_{xK}}}$, is plotted. It is expected that about 95 percent of the estimates will fall inside these bounds. As can been seen in Fig 34, most of the estimates calculated from the moving window do

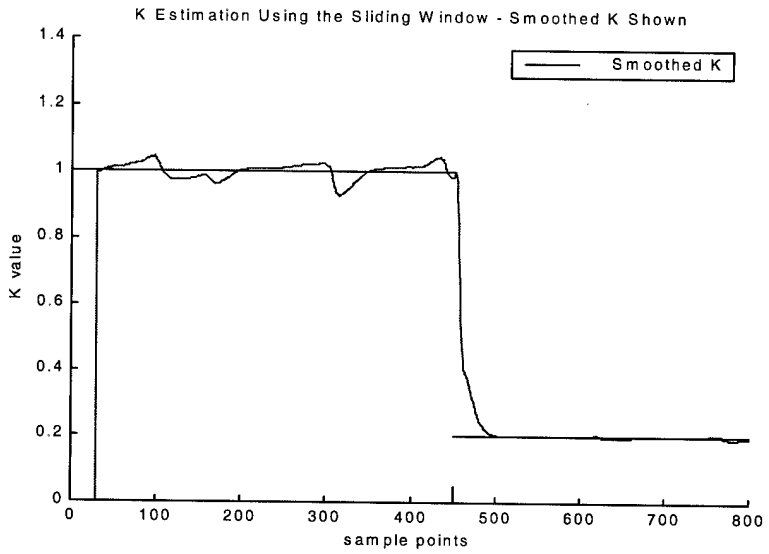

Figure 32. Moving window loop gain estimate; K_1=0.2, $\sigma_q = 0.01108\,\text{deg/sec}$, $\sigma_\alpha = 0.03\,\text{deg}$ and SNR=53.286 dB

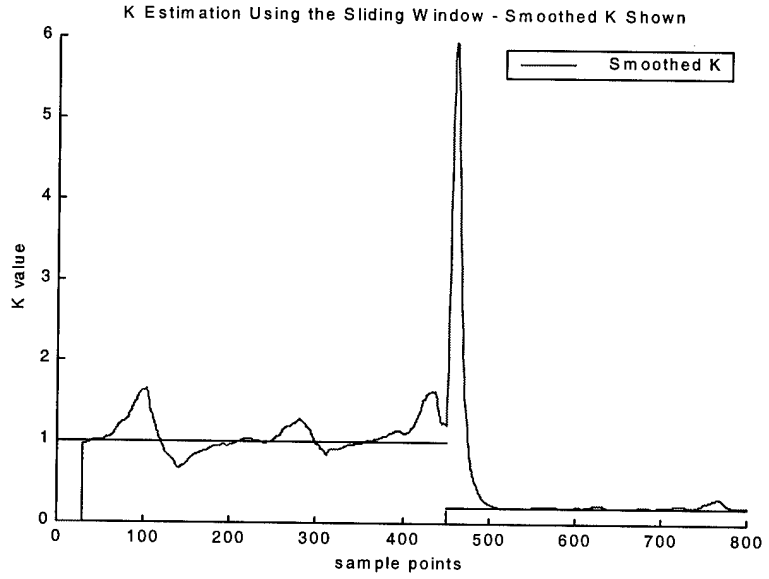

Figure 33. Moving window loop gain estimate; K_1=0.2, $\sigma_q = 0.555\,\text{deg/sec}$, $\sigma_\alpha = 0.03\,\text{deg}$ and SNR=23.29 dB

fall within these bounds. When the error covariance of the open-loop gain is large, the estimates from moving window identification algorithm are poor. This occurs when there are high dynamic changes of the input command. Indeed, Theorem 1 provides a rigorous open-loop gain estimation algorithm. Hence, as expected, Fig. 34 amply illustrates that "Kalman filter divergence" does not occur, i.e., our open-loop estimate is indeed reliable.

Obviously, K is within the limits of 1 and 0, 1 for no failure and 0 for a complete loss of control surface area. As shown in Figs. 33,32, 36 and 38, the loop gain estimates before the point of failure often exceeded K_1=1. We know that this can not be the case. The plant's open-loop gain estimates provided by our smoothed moving window system identification algorithm can be modified using the above upper and lower bound information: when the moving window's identified loop gain estimates are greater than one or less than zero, they are set equal to their respective limits. This will reduce the estimated loop gain fluctuations before they are smoothed.

After limiting the loop gain value estimate to 1 for the case when the SNR = 23.29 dB and the degree of failure is $K_1 = 0.2$, the open-loop gain identification performance, shown in Fig. 35, is obtained - compare to Fig. 33.

For the simulation runs presented in Figs. 36-39, both the α and q measurement noise intensity was varied according to Eqs. (83a) and (83b). As can be seen, as the SNR increases from 23 dB to 40 dB, there is a significant improvement in the system identification algorithm's ability to estimate the open-loop gain accurately. For lower values of SNR, a moving window with a larger sample size would be needed to obtain more accurate results. However, as shown in the next Section, even with poor open-loop gain estimates, when adaptive control is implemented, tracking performance is restored.

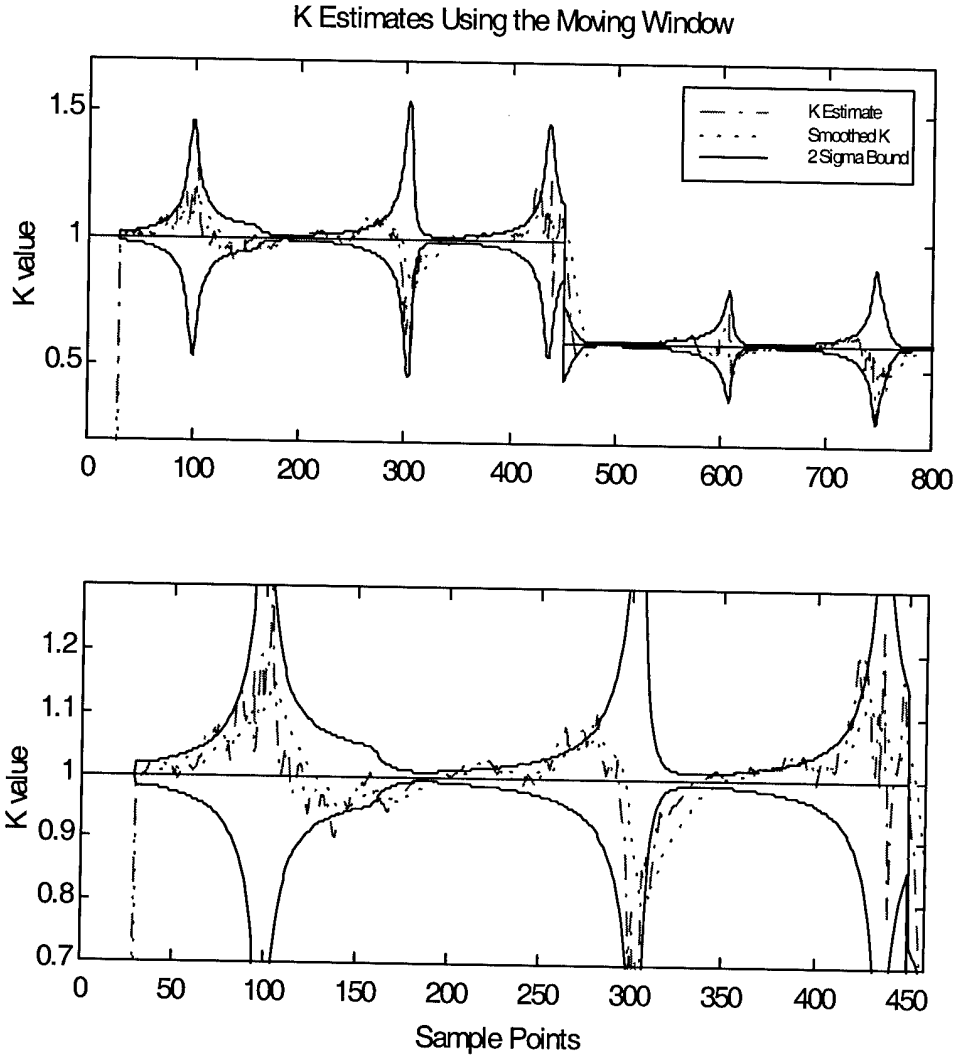

Figure 34. Two sigma analysis of moving window estimates; K_1=0.6, $\sigma_q = 0.1108\,\text{deg/sec}$, $\sigma_\alpha = 0.03\,\text{deg}$ and SNR=37.277 dB

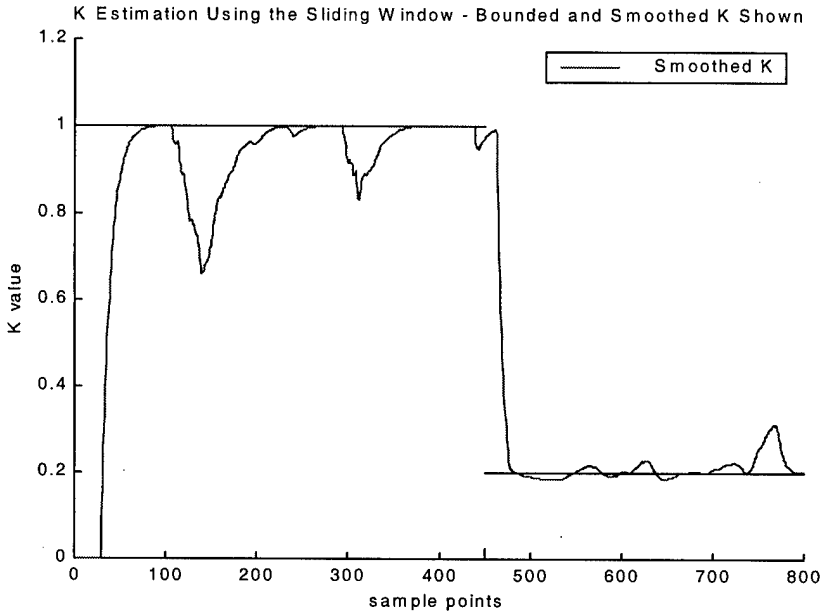

Figure 35. Loop gain estimate with upper and lower bounds; K_1=0.2, $\sigma_q = 0.555\,\text{deg/sec}$, $\sigma_\alpha = 0.03\,\text{deg}$ and SNR=23.29 dB

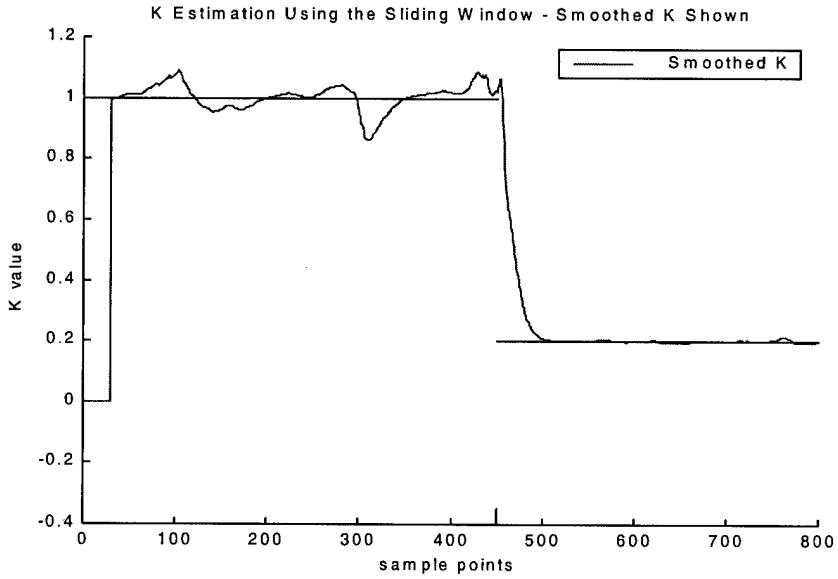

Figure 36. Moving window loop gain estimate; K_1=0.2, $\sigma_q = 0.0739\,\text{deg/sec}$, $\sigma_\alpha = 0.0739\,\text{deg}$ and SNR=40 dB

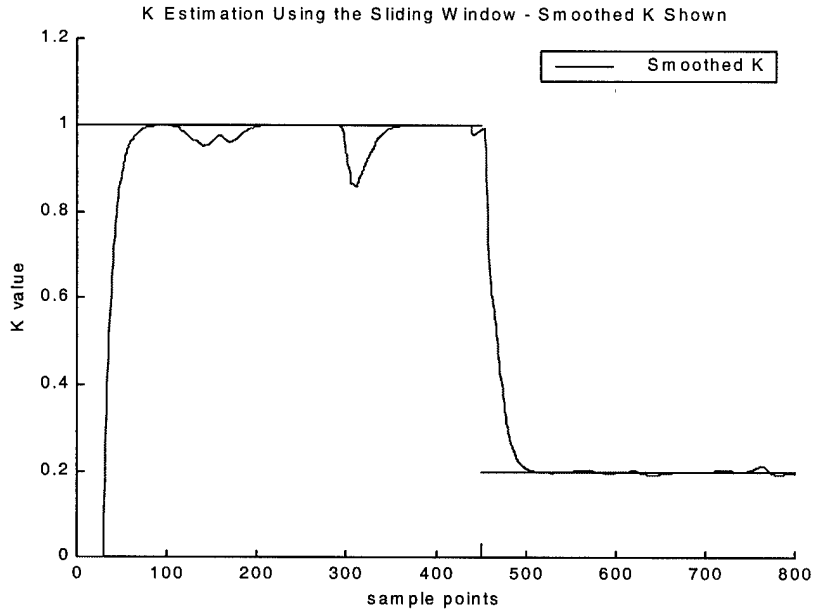

Figure 37. Loop gain estimate with upper and lower bounds; K_1=0.2, $\sigma_q = 0.0739\,\text{deg/sec}$, $\sigma_\alpha = 0.0739\,\text{deg}$ and SNR=40 dB

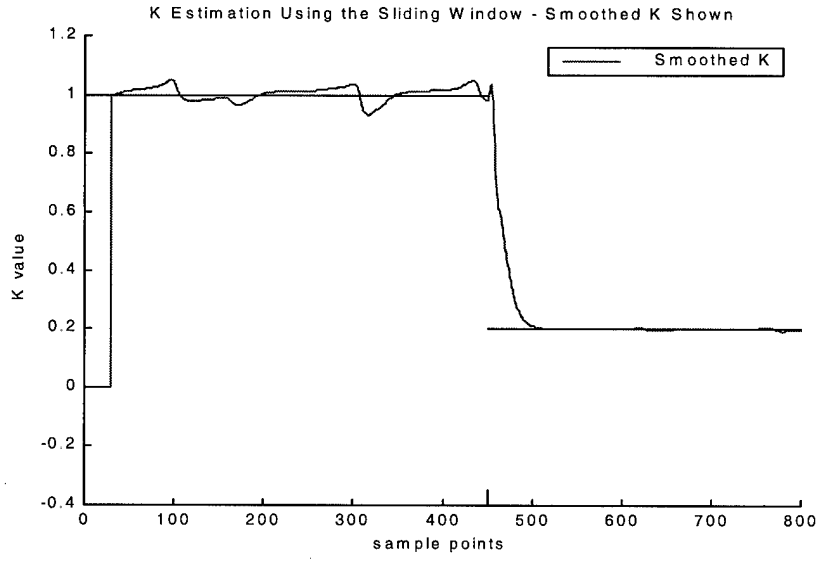

Figure 38. Moving window loop gain estimate; K_1=0.2, $\sigma_q = 0.00739\,\text{deg/sec}$, $\sigma_\alpha = 0.00739\,\text{deg}$ and SNR=60 dB

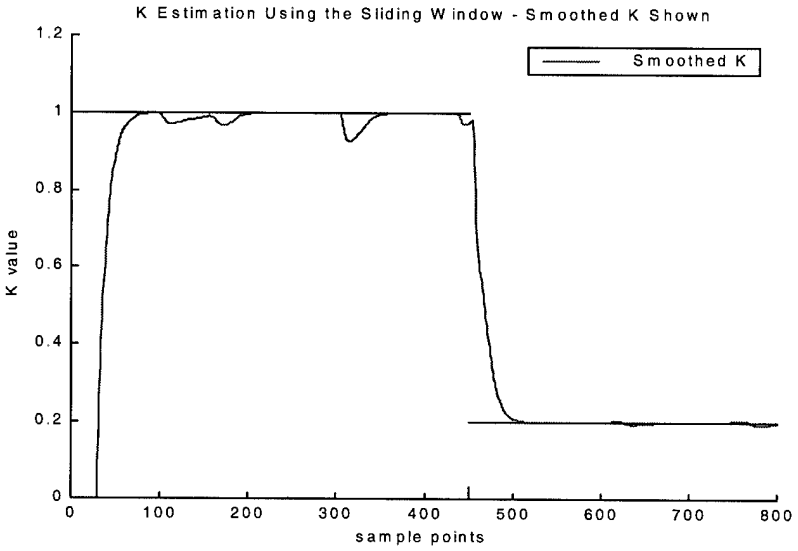

Figure 39. Loop gain estimate with upper and lower bounds; K_1=0.2, $\sigma_q = 0.00739\,\text{deg}/\text{sec}$, $\sigma_\alpha = 0.00739\,\text{deg}$ and SNR=60 dB

5.6 Indirect Adaptive Control

The loop gain estimates are now used on-line to correct for the failure. In our indirect adaptive control mechanization, the reciprocal of the open-loop gain estimate is continuously fed back into the controller, as shown in Fig. 1. By doing so, the failure is taken into account and it is to be expected that the control system will respond as if a failure never happened. Using the K estimates obtained under the same low SNR conditions as in Figs. 33 and 35, the post failure tracking performance is improved - see e.g., Figs. 40 and 41, respectively.

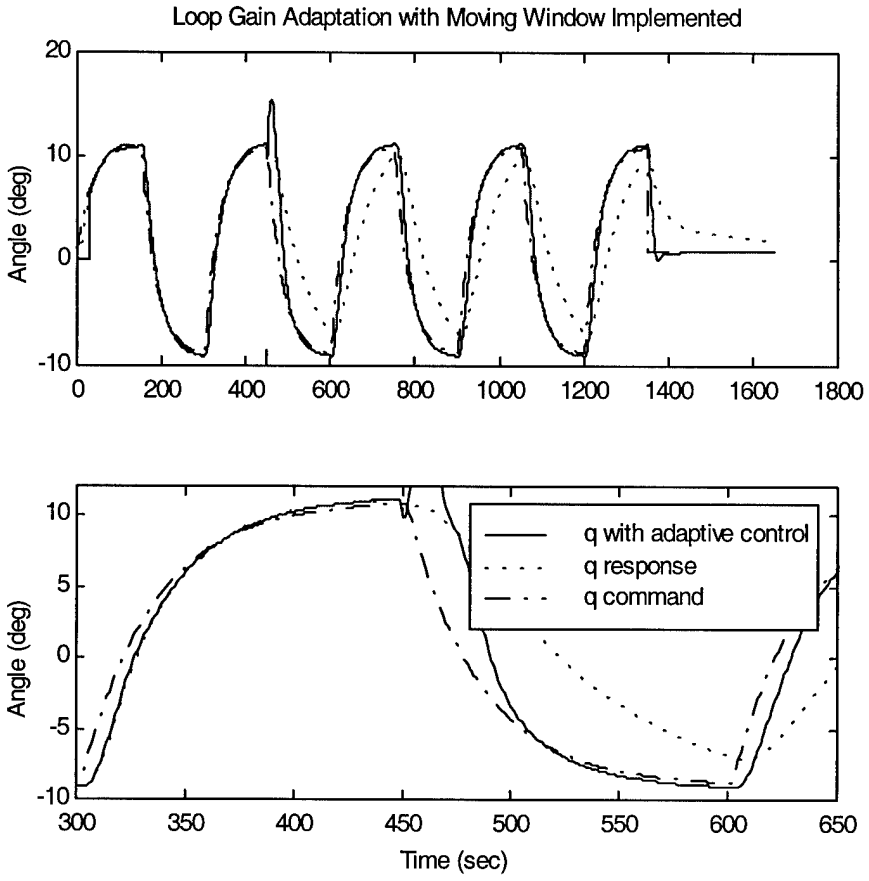

Figure 40. Pitch rate tracking with failure and K adaptation; K=0.2, $\sigma_q = 0.555\,\text{deg}/\text{sec}$, $\sigma_\alpha = 0.03\,\text{deg}$ and SNR=23.29 dB

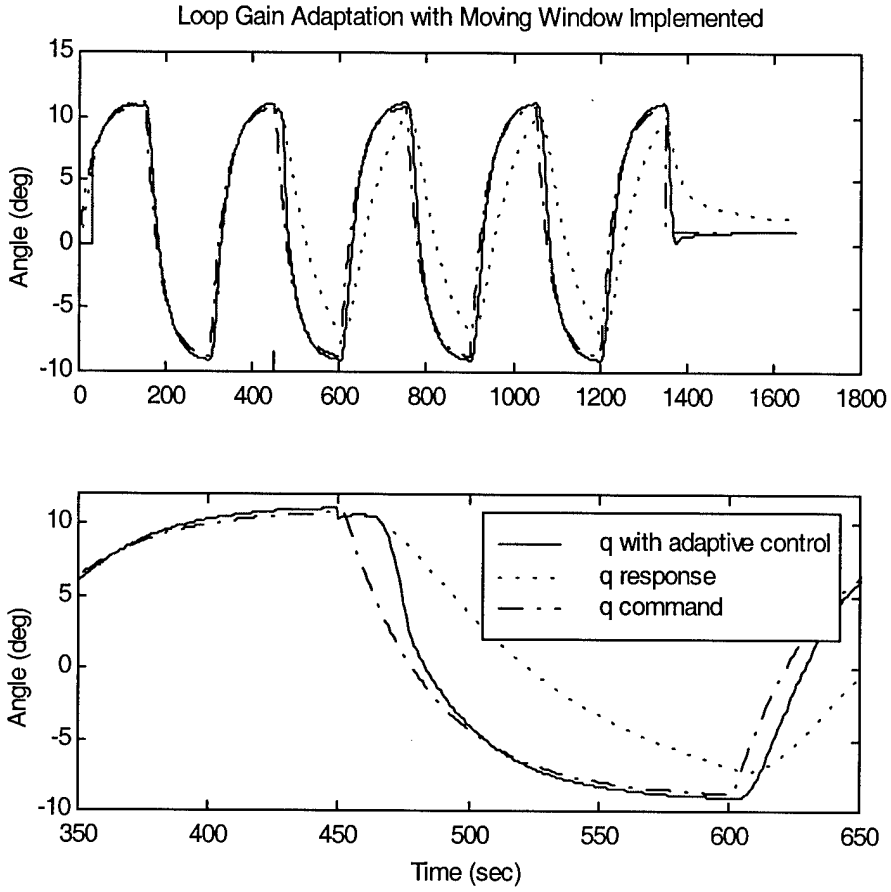

Figure 41. Pitch rate tracking with failure and K adaptation using upper and lower bounds; K_1=0.2, $\sigma_q = 0.555\,\mathrm{deg}/\mathrm{sec}$, $\sigma_\alpha = 0.03\,\mathrm{deg}$ and SNR=23.29 dB

Figs. 42 and 43 demonstrate this point for an extreme degree of failure of K_1=0.2, in which case, we recall, the fixed controllers could not cause the system output to track the reference command properly (see, e.g., Fig. 17). In addition, a relatively low SNR of 37.227 dB is used in this experiment. Note, that in Fig. 42, the estimate is significantly worse around the failure point than

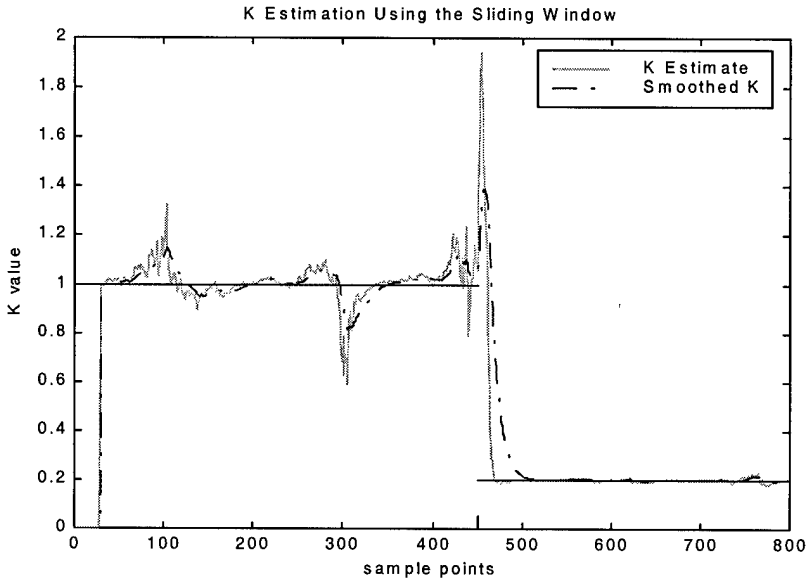

Figure 42. Open-loop gain estimation using a moving window when K_1=0.2 and SNR=37.227 dB

in Fig. 31 when the degree of failure was K_1=0.6. Thus, the degree of failure directly impacts the loop gain estimation performance near the instant of failure. Also, the peaks in estimation error occur near the peaks of the input signal.

In Figs. 14-18, it was shown that, for a high degree of failure, the tracking performance deteriorates. However, the K estimation error peaks are smaller when there is a reduction in tracking performance. This trend is evident in Figs. 33, 36 and 38 where the estimation performance after the failure, where tracking is poor, is consistently better than before the failure. In addition, the higher the degree of failure and the poorer the tracking performance provided by the fixed controller, the better the esitmation performance. Moreover, Fig. 44 shows the loop gain estimates

after the adaptive controller is implemented and tracking performance is restored after the failure. As can be seen, there is a significant reduction in estimation performance due to the reduction in excitation when tracking is restored - compare Figs. 42 and 44. Now, even though there are numerous instances of poor estimation, when the smoothed and bounded loop gain estimate $\hat{K}$ is used modify the controller, the ensuing tracking performance of the adaptive controller is excellent as shown in Figs. 41, 43 and 45-47.

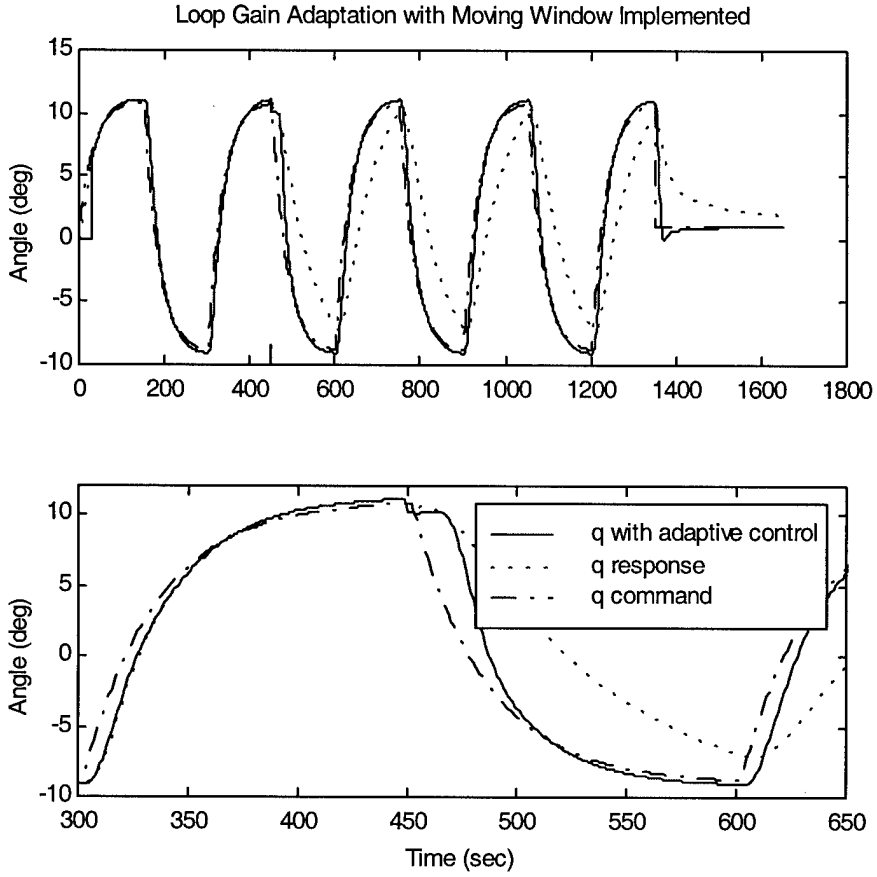

Figure 43. Pitch rate response comparison with and without K adaptation; K_1=0.2, $\sigma_q = 0.1108\,\text{deg}/\text{sec}$, $\sigma_\alpha = 0.03\,\text{deg}$ and SNR=37.227 dB

The adaptive control system's tracking performance at the higher SNRs of 40, 53.286 and 60 dB is shown in Figs. 45-47.

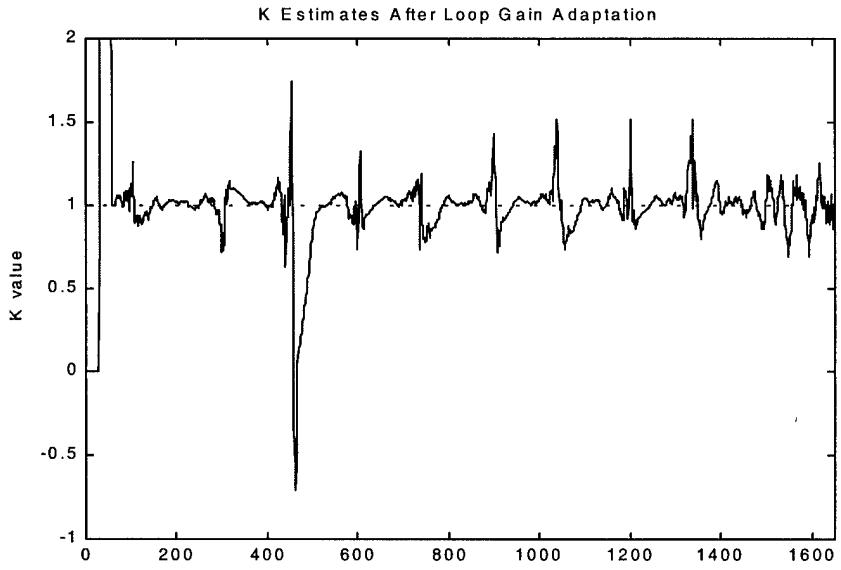

Figure 44. K estimates after loop gain adaptation; K_1=0.2, $\sigma_q = 0.1108\,\text{deg}/\text{sec}$, $\sigma_\alpha = 0.03\,\text{deg}$ and SNR=37.227 dB

In conclusion: Figs. 40, 41, 43 and 45-47 were all created by calculating the loop gain estimate over each time epoch following which the reciprocal of the loop gain is fed back, as shown in Figure 1. In addition, α and q are also estimated for each epoch bu the system identification algorithm and are then fed to the feedback controller. This produces the q output signal described above as 'q with adaptive control'. For a high degree of failure and before the loop gain was adapted, the fixed controllers could not track properly. Once an adaptive tracking controller is implemented and the effective loop gain is restored, tracking performance is recovered. In addition, when the bound limited open-loop gain estimate is used in the adaptive control algorithm, the hump in q at $t = 4.5+$ seconds is removed, as shown in Figs. 40-41.

In summary, as the degree of failure increased, the systems' ability to track the command input deteriorated. When the degree of failure was low, $K_1 = 0.25$, tracking performance no longer was considered acceptable. The system identification algorithm was applied to an F-16 class control system and the states and loop gain were jointly estimated. To improve failure detection time, a moving window algorithm was created to estimate the loop gain. The loop gain estimates fluctuated appreciable from their true value. To reduce the fluctions, a smoothing filter was introduced. The smoothed loop gain estimates were then applied to the indirect adaptive controller to correct the failure in the system and make the tracking response appear as if the failure never happened. The results were excellent.

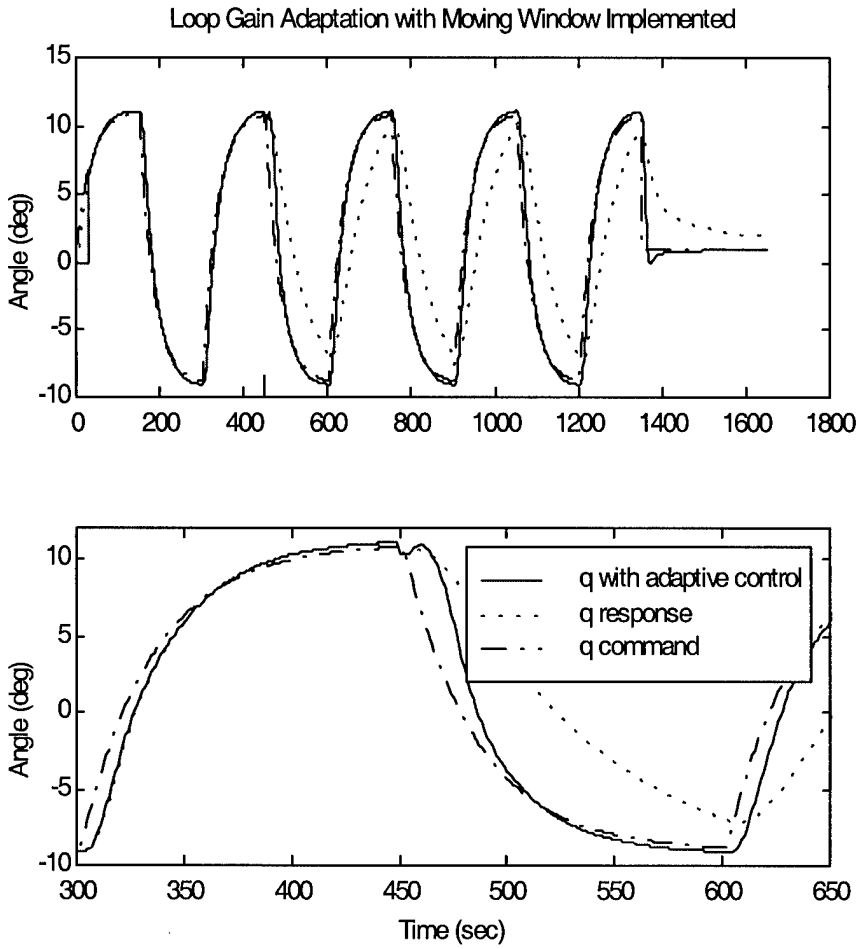

Figure 45. Pitch rate tracking with failure and K adaptation using upper and lower bounds; K_1=0.2, $\sigma_q = 0.0739\,\mathrm{deg}/\mathrm{sec}$, $\sigma_\alpha = 0.0739\,\mathrm{deg}$ and SNR=40 dB

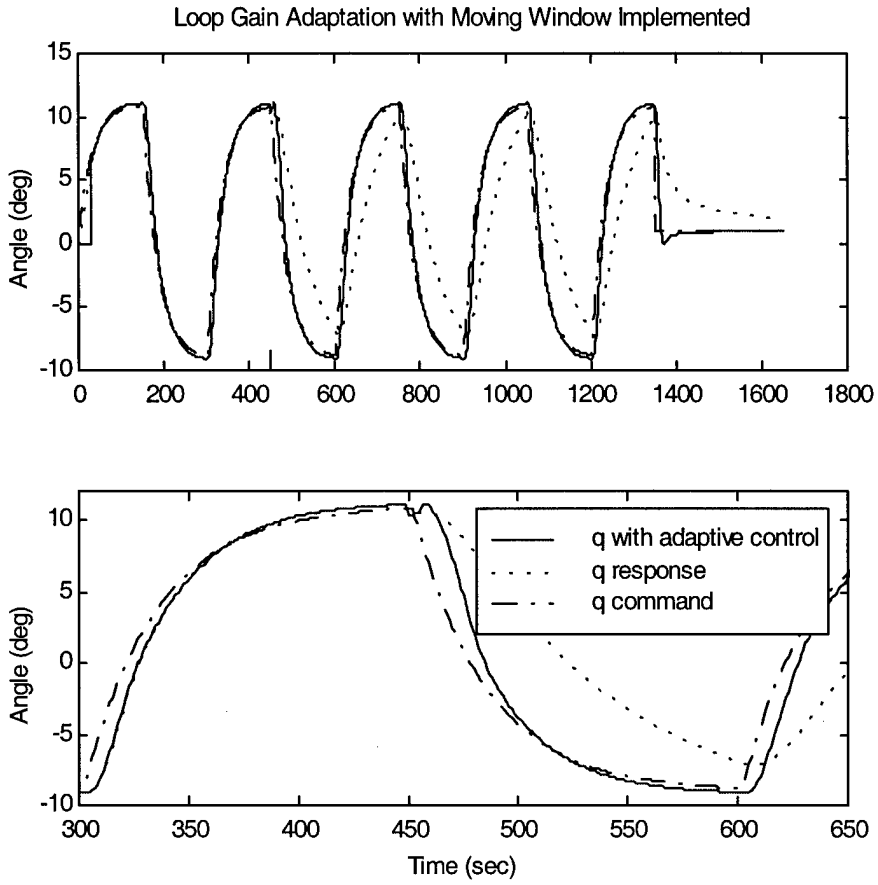

Figure 46. Pitch rate tracking with failure and K adaptation; K_1=0.2, $\sigma_q = 0.01108\,\text{deg}/\text{sec}$, $\sigma_\alpha = 0.03\,\text{deg}$ and SNR=53.286 dB

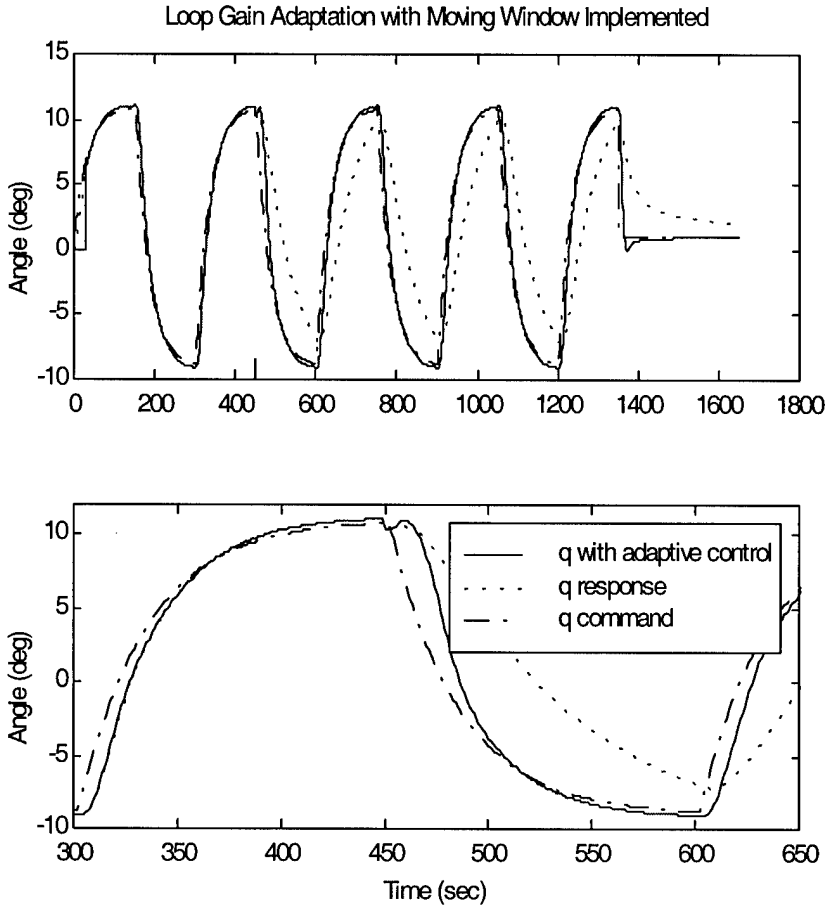

Figure 47. Pitch rate tracking with failure and K adaptation using upper and lower bounds; K_1=0.2, $\sigma_q = 0.00739\,\text{deg}/\text{sec}$, $\sigma_\alpha = 0.00739\,\text{deg}$ and SNR=60 dB

Chapter 6 - Conclusions and Recommendations

6.1 Summary

Chapter 2 of this thesis described how system identification techniques can determine the unknown parameters of a model. We began with modeling disturbances and the importance of not over-modeling an unknown system. A classical system identification approach for solving the unknown parameters of an n^{th} order SISO system was given. The approach was then demonstrated using a second order example. The example assumed there was an absence of measurement noise. When determining the proper model of the dynamic system, the applied input must have an order equal to or greater than the number of unknown parameters. For this reason, we chose n sinusoidal test functions. Each sinusoid produces 2n equations needed to solve the unknown parameters of the n^{th} order SISO system. Chapter 2 also provided the case when measurement noise was an influence on the modeling of a dynamic system. Because of the measurement noise, a stochastic approach was then introduced, defining the Least Squares algorithm. It was then shown how the strength of the noise can be represented as a weighting matrix, R, and applied to the state estimates to provide more accurate results.

Next, Chapter 3 described the plant used in this thesis. Only the deterministic approach was identified. It was important to dismiss the process and measurement noise initially. The absence of the noise allowed us to see the true response of the system and determine if any additional considerations were needed regarding the model. This chapter also presented the methods used to augment the state matrix and the appropriate control laws were defined. We saw that the tracking of the system was not adequate. To compensate for the steady state error, both a PI controller and a proportional controller were described and implemented to represent two different simulation scenarios.

In summary, a system identification algorithm was developed to identify a systems' loop gain, K. A proof of this theorem, was given and supporting examples discussed. An alternative batch approach to loop gain estimation was also given.

The recursive system identification algorithm was described in Chapter 4. The algorithm used Kalman filtering techniques to measure and estimate the state outputs, α and q (angle of attack and pitch rate respectively), and the critical loop gain, K. We then assumed that our measurement devices were not perfect and noise was being injected into the α and q channels. The Kalman equations were manipulated so that the loop gain can be estimated. Once the identification algorithm was complete, a simple example was provided to test the validity of Theorem 1, the system identification algorithm. In addition to the recursive identification algorithm, a batch estimation algorithm was also provided but not explored.

Finally, Chapter 5 confirmed the functionality of the proposed system identification algorithm. The algorithm is tested for both the PI controller and the proportional controller. In this chapter the expanding horizon Kalman estimates were compared to the estimates from the moving window. The performance of both methods were analyzed and compared for their ability to predict a failure. Since the algorithm is a function, in some part, of the measurement noise, the SNR was varied so the effects of noise on the system could be analyzed. When the moving window was implemented, spots of poorer estimation were observed. To help correct this, a smoothing function was used and tested for different smoothing percentages. The reciprocal of the estimated loop gain derived from the system identification algorithm was then fed back recursively to provide a continuous correction factor to the failed plant. This was done over different SNRs and failure amounts.

6.2 Conclusion

An algorithm for the identification of a control system's loop gain, K, is presented. The derived algorithm yields joint estimates for both the system's state and the open-loop gain. The open-loop gain and state estimation algorithm is being referred to as the system identification algorithm.

Using state feedback, the original unstable plant of the F-16 class aircraft could be made stable. A PI controller or a proportional gain controller needed to be added to correct the steady state error of the pitch rate tracking. The final plants' tracking performance was tested using various failure amounts: $K_1 = 0.8$, 0.6, 0.4, 0.2 and 0.1. Tracking performance began to slightly degrade at a degree of failure $K_1 = 0.6$. As the degree of failure increased, the tracking performance decreased. When the loop gain $K_1 = 0.25$, tracking was no longer acceptable. Even though tracking is no longer acceptable at $K_1 = 0.25$ the plant was able to tolerate a failure of $K_1 = 0.08$ before coming unstable again. Since the original plant was robust, it didn't matter much which controller was used, the PI or the proportional gain controllers. Both controllers, when implemented and ran, provided near identical test results. For this simulation, only one consistent command input signal was tested.

It was also shown that a moving window can provide faster detection times for failure than the continuously expanding Kalman filter. The moving window used in this thesis had a length of thirty samples or 0.3 seconds. The initial state and loop gain values, $\alpha = -1.4414$ [deg], $q = -2.4314$ [deg/sec], $K_1 = 0.8$, and the variances, 0.1 [deg^2], 1 [(deg/sec)^2] and 0.4, were updated before each run. There were times when some windows provided estimates that jumped appreciably from their expected values. This occurred around the high dynamic change of the input signal, when the input wave was at its highest or lowest peak. When the window size was increased, the estimate fluctuations decreased. However, a shorter window was able to detect a failure faster larger window, which is desirable.

To reduce the size of the fluctuations without increasing the window length, a smoothing filter was used. The moving window reduced the fluctuations but also increased the detection time of the failure. It was demonstrated that the more the estimates were smoothed, the longer it took to detect the failure amount. The 90 % smoothed estimates still detected the failure faster than the continuously expanding Kalman filter. These smoothed estimates were used for the rest of the simulation.

With the moving window estimation algorithm, the quality and accuracy of the results depended greatly on the quality of the measurements. This is a result of the short amount of time used to calculate the estimates. When the SNR became low, signifying more noise in the system, the loop gain estimates fluctuated from the true failure amount. That is, there was a higher range of values for the loop gain estimates when the SNR was low than when it was higher. This deviation, for when the moving window was implemented, was on the order of $K \pm 0.35$ before the onset of failure at $t = 4.5$ sec and a SNR $= 37$ dB. In contrast, the estimates after the failure fluctuated less and as the degree of failure increased, the fluctuations decreased even further. This was contributed to the additional excitation created by the low failure, which in turn, caused poor tracking. It is evident that excitation of the plant parameters is important to system identification.

All the research so far was to test the stability of the plant and the accuracy of the identification algorithm. Once the system identification algorithm calculated the loop gain, its reciprocal was fed back to correct the failure. The results are excellent. The identification algorithm was capable of detecting the loop gain at all failure amounts. Even when the plant model could no longer track the command input, the algorithm still provided accurate estimates. This is when the feedback is most critical. It was shown that when the estimates were used in the feedback path for low failures, when the system no longer tracked, the result was nearly complete correction of the failure.

However, for low SNR and high degree of failure the estimates from the moving window fluctuated greatly around the failure point, $\hat{K} \approx 6$, causing the adaptive controller to track the command input improperly. The degree of failure was defined as being within the range of 1 and 0, 1 for no failure and 0 for complete loss of actuator control. The moving window frequently estimated the loop gain as falling outside these bounds, especially before the point of failure. To correct this, the estimates were set equal to the respective bound that the estimate broke. When these bounded estimates were applied to the adaptive controller, improved tracking could be seen. The improvement of the system was significant.

In summary, the loop gain of a dynamic system can be found and applied to an indirect adaptive controller to compensate for actuator failure.

6.3 Recommendations for Future Research

The research presented used only a single input signal and the short period approximation of an F-16 class aircraft. The algorithm should be applied to the full scale aircraft system equations. It should then be followed up using various input signals to test the algorithm at different levels of excitation. Also one can create a scenario when the B matrix is changed to do structural damage.

When simulating the failure of the elevator control surface, no process noise or external disturbance is injected into the model. Process noise and a disturbance noise should be added into the model. A constant noise vector was used. Instead, running a Monte Carlo run to obtain a random noise vector would be more realistic. Also, instead of performing a single error run, it would be better to show mean and 1 sigma time histories for 10-25 Monte Carlo runs. This would give a greater insight on how the adaptive controller is performing.

Most of the simulation was done non-real-time. A new simulation code could be developed to simulate the failure real-time and correct real-time.

Another study could be created under the flight condition of straight and level. This would require using a dither to enhance estimation.

Bibliography

[1] Brown, J. M, II. *Optimal Inputs for System Identification.* PhD dissertation, AFIT/DSG/ENG/95-S-04, School of Engineering, The Air Force Institute of Technology, Wright-Patterson AFB, OH, September 1995.

[2] Caglayan, A. K., et. al. "Detection, Identification and Estimation of Surface Damage/Actuator Failure for High Performance Aircraft." Poceedings of the 7th American Control Conference, Atlanta, Georgia, June 1998, pp. 2206-2212.

[3] Chandler, P., et. al. "On-Line Optimizing Networks for Reconfigurable Control." Proceeding of the 32nd Conference on Decision and Control, San Antonio, Texas, December 1993, pp. 2272-2277.

[4] Chandler, P., et. al. "Constrained Linear Regression for Flight Control System Failure Identification." Proceedings of the American Control Conference, San Francisco, California, June 1993, pp. 3141-3145.

[5] Chandler, P., et. al. "Regression Techniques for Aircraft Parameter Identification from Noisy Measurements in maneuvering Flight." Proceedings of the 31st Conference on Decision and Control, Tucson, Arizona, December 1992, pp. 2311-2316.

[6] Chandler, P., et. al. "System Identification for Adaptive and Reconfigurable Control." Journal of Guidance, Control and Dynamics, Vol. 18, No. 3, June 1995, pp. 516-524.

[7] Chen, Han-Fu. "Recursive Estimation and Control for Stochastic Systems." New York: John Wiley and Sons, Inc., 1985.

[8] D'Azzo, John, J. and Constantine H. Houpis. "Linear Control Systems Analysis and Design: Conventional and Modern (4th edition)." New York: McGraw-Hill, Inc., 1995.

[9] Franklin, Gene F. "Digital Control of Dynamic Systems (3rd edition)." Menlo Park, California: Addison Wesley Longman, Inc., 1998.

[10] Houpis, C. H. and Mier Pachter. "Application of QFT to Control System Design-An Outline for Engineers." International Journal of Robust and Nonlinear Control, Vol. 7, No 6, June 1997, pp. 515-531.

[11] Ljung, L. "System Identification for the User." Prentice Hall, 1987.

[12] The MathWork, Inc., 21 Elliot Street, Natick, MA 01760. MATLAB. December 1997. Version 5.2.

[13] Maybeck, P. "Stochastic Models, Estimation and Control, Volume 1." Arlington, VA: Navtech Book and Software Store, 1994.

[14] Maybeck, P. "Stochastic Models, Estimation and Control, Volume 2." Arlington, VA: Navtech Book and Software Store, 1994.

[15] Norton, J. P., "An Introduction to Identification." London: Academic Press, 1986.

[16] Pachter, M. *Class notes from EENG 640: Flight Dynamics I*. The Air Force Institute of Technology, Wright-Patterson AFB, OH, 1998.

[17] Pachter, M. *Class notes from EENG 708: Multivariable Systems*. The Air Force Institute of Technology, Wright-Patterson AFB, OH, 1998.

[18] Pachter, M., et. al. "Control Reconfiguration with Actuator Rate Saturation." Proceedings of the 14th American Control Conference, Seattle Washington, June 1995, pp. 3495-3499.

[19] Pachter, M., et. al. "Reconfigurable Tracking Control with Saturation." Journal of Guidance, Control and Dynamics, Vol. 18, No. 5, Sept-Oct 1995, pp. 1016-1022.

Vita

Lieutenant Jamey Sillence was born on 4 April 1975 in Smithtown, New York. He graduated in 1993 from Seaford High School, Seaford, New York. He graduated with distinction from Clarkson University in 1997 with a Bachelors of Science degree in Electrical Engineering. Lieutenant Sillence, being a distinguished graduate from the ROTC, received a commission into the United States Air Force upon graduation. His first assignment was to go direct assession to the AFIT masters program. His course work was completed March 1999. His follow-on assignment is to Holloman AFB, NM, working for the 746th Test Squadron.

REPORT DOCUMENTATION PAGE

Form Approved
OMB No. 0704-0188

1. AGENCY USE ONLY *(Leave blank)*	2. REPORT DATE	3. REPORT TYPE AND DATES COVERED
	March 1999	Thesis

4. TITLE AND SUBTITLE
Loop Gain Estimation for Adaptive Control

5. FUNDING NUMBERS

6. AUTHOR(S)
Jamey P. Sillence
Second Lieutenant, USAF

7. PERFORMING ORGANIZATION NAME(S) AND ADDRESS(ES)
The Air Force Institute of Technology
2950 P Street
Wright-Patterson AFB, OH 45433-7765

8. PERFORMING ORGANIZATION REPORT NUMBER
AFIT/GE/ENG/99M-27

9. SPONSORING/MONITORING AGENCY NAME(S) AND ADDRESS(ES)
Dr. Siva Banda/Aeronautical Engineer
2210 8th Street
Bldg 146
Wright-Patterson AFB, OH 45433
(937) 255-8677

10. SPONSORING/MONITORING AGENCY REPORT NUMBER

11. SUPPLEMENTARY NOTES

12a. DISTRIBUTION AVAILABILITY STATEMENT
Approved for public release; distribution unlimited

12b. DISTRIBUTION CODE

13. ABSTRACT *(Maximum 200 words)*

The identification of a linear discrete-time control system's loop gain is addressed. The classical Kalman filter theory for state estimation in linear control systems is extended, and the control system's loop gain and states are jointly estimated. A rigorous analysis of the measurement situation on hand yields explicit formulae for the loop gain's unbiased estimate and estimation error's convariance.

14. SUBJECT TERMS
system identification, adaptive control

15. NUMBER OF PAGES
100

16. PRICE CODE

17. SECURITY CLASSIFICATION OF REPORT	18. SECURITY CLASSIFICATION OF THIS PAGE	19. SECURITY CLASSIFICATION OF ABSTRACT	20. LIMITATION OF ABSTRACT
unclassified	unclassified	unclassified	UL